Supporting Information for

Synthesis of bright water-soluble circularly polarized luminescence emitters as potential sensors

Joseph A. Adewuyi[a], Nathan D. Schley[b], Gaël Ung*[a]

[a]Department of Chemistry, University of Connecticut, Storrs, Connecticut 06269, United States.

[b]Department of Chemistry, Vanderbilt University, Nashville, Tennessee 37235, United States.

E-mail: gael.ung@uconn.edu

Table of Contents

General Methods and Material:
The ligand synthesis was carried out using standard Schlenk techniques. However, the lanthanide complexes were synthesized under atmospheric conditions. The $La(NO_3)_3{\cdot}6H_2O$ was purchased from Fluka Analytical. The $Tb(NO_3)_3{\cdot}6H_2O$ and $Eu(NO_3)_3{\cdot}6H_2O$ were purchased from Strem Chemicals. The $Dy(NO_3)_3{\cdot}xH_2O$, KOH, and K_2CO_3 were purchased from Sigma-Aldrich. The $Sm(NO_3)_3{\cdot}6H_2O$ was purchased from Acros Organics.

NMR Spectroscopy. All NMR spectra were recorded on a Bruker AVANCE III 400 MHz spectrometer. The spectra were processed using MestReNova and Bruker TopSpin softwares. Chemical shifts are reported in parts per million (ppm) and were determined relative to the residual solvent signal (4.79 ppm for D_2O)

Photophysical Studies. All photophysical studies were performed in sealed cuvettes under atmospheric conditions using 0.1 M tris buffer (pH 7.4) as solvent. Absorbance, excitation, and emission spectra were recorded on a HORIBA Duetta Spectrophotometer using HORIBA EzSpec Software. Absorbance spectrum was measured at 3.0×10^{-5} M, while excitation and emission spectra were measured at 6.1×10^{-4} M. Circularly polarized luminescence was measured on an OLIS CPL Solo set at 1 sec integration time with 6.1×10^{-4} M solutions. Metal cation (Pb^{2+}, Cd^{2+}, Mn^{2+}) and pH titrations were measured at 6.1×10^{-5} M of the lanthanide complex. Quantum yields were determined by relative method with 9,10-diphenylanthracene ($\Phi = 0.86$ in cyclohexane) as the standard on a HORIBA Duetta Spectrophotometer using HORIBA EzSpec Software. Lifetimes were recorded from 6.1×10^{-4} M solutions using an OLIS CPL Solo spectrofluorometer; spectra were collected using pulsed excitation at 280 nm (for pH titration experiment, a 490 nm LED was used) and time-resolved emission measurements fixed at the peak of strongest emission. A first order exponential decay curve was fit to the collected data to estimate the fluorescence lifetime (τ_{obs}). Values are reported as measured lifetimes (observation wavelength). The number of coordinated water molecules was calculated from lifetime measurements for Tb and Eu using Parker's equation, $q = A_{Ln}(1/\tau_{H2O} - 1/\tau_{D2O} - \alpha_{Ln})$ with $A_{Tb} = 5$ ms, $A_{Eu} = 1.2$ ms, $\alpha_{Tb} = 0.06$ ms^{-1}, and $\alpha_{Eu} = 0.25$ ms^{-1}.

XRD Studies. Single-crystal X-ray diffraction studies were performed at Vanderbilt University. Single crystals were developed by slow evaporation of concentrated aqueous solution of the europium complex. A suitable crystal was selected for analysis and mounted in a polyimide loop. All measurements were made on a Rigaku Oxford Diffraction Supernova Eos CCD with filtered Mo Kα radiation at a temperature of 100 K. Using Olex2.36, the structure was determined with the ShelXL structure solution program using direct methods and refined with the ShelXL refinement package37 using least-squares minimization.

pH Measurement. pH of the aqueous solutions was measured with the aid of a calibrated Orion Star A2111 benchtop pH meter made by Thermo Fisher Scientific.

Mass Spectrometry. High resolution mass spectrometry was conducted for the complexes using an Applied Biosystems Sciex Qstar Elite LC mass spectrometer. The samples were prepared in a water: methanol (1:9) solvent system at 5 x 10^{-5} M concentration.

Synthesis of *N,N,N',N'*-tetrakis[6-carboxypyridin-2-yl)methyl]diaminocyclohexane (H_4tpadac).

The synthesis was performed analogous to that reported for the achiral ligand.[1]

To a flame-dried Schlenk tube, a solution of 6-bromomethylpyridine-2-carboxylic acid methyl ester (560 mg, 2.434 mmol) in dry acetonitrile (10 mL) was added, then a solution of enantiopure diaminocyclohexane (65 mg, 0.562 mmol) in 10 mL dry acetonitrile and then anhydrous K_2CO_3 (503 mg, 3.642 mmol) was added under a flow of nitrogen. The reaction was refluxed for 48 h. The solvent was then removed *in vacuo* to obtain a light brown solid. The solid residue was dissolved in dichloromethane (40 mL) then washed with water (3 x 40 mL) and dried over anhydrous Na_2SO_4. The solvent was then removed *in vacuo* and a light brown oil was obtained. The crude oil was refluxed in 5 M HCl overnight. Afterwards, the solvent was evaporated. 1 M HCl (4 mL) was added to give an aqueous solution to which acetone (100 mL) was added while stirring to precipitate the hydrochloride salt of the ligand as an off-white solid with a yield of 45% over two steps. ^{1}H NMR (D_2O, 400 MHz): δ (ppm): 1.51 ppm (br, 2H), 1.75 ppm (br, 2H), 2.01 ppm (br, 2H), 2.16 ppm (br, 2H), 2.48 ppm (br, 2H), 4.13 ppm (d, 4H), 4.36 ppm (d, 4H), 7.42 ppm (br, 4H), 7.87 ppm (br, 8H).

General procedure for the synthesis of [(tpadac)Ln][K]

To a solution of enantiopure H_4tpadac·6HCl·5H_2O (0.1 g, 0.1038 mmol) in water (3 mL), 0.2 M KOH was added until the pH reached 7. Then a solution of the lanthanide salt (0.1038 mmol) in water (0.0346 M) was added. The pH was then readjusted to 7 using 0.2 M KOH, and the reaction was stirred overnight. Afterwards, the solvent was evaporated *in vacuo* then the residue was dissolved in ethanol (20 mL), which was then sonicated. The ethanol solution was filtered, and the filtrate was evaporated to obtain the desired lanthanide complex as a white solid.

Synthesis of [(*R,R*-tpadac)La][K]

Following general procedure, a white solid was obtained. ^{1}H NMR (D_2O, 400 MHz): δ (ppm): 1.07 (br, 2H), 1.60 (br, 2H), 1.77 (br, 2H), 2.07 (br, 2H), 2.48 (br, 2H), 3.19 (d, *J* = 15.6 Hz, 2H), 3.68 (d, *J* = 16.4 Hz, 2H), 4.12 (2d, *J* = 20.5, 16.1 Hz, 4H), 7.37 (d, *J* = 7.6 Hz, 2H), 7.44 (d, *J* = 7.6 Hz, 2H), 7.76 (d, *J* = 7.7 Hz, 2H), 7.93 (dt, *J* = 33.5, 7.1 Hz, 6H).

Synthesis of [(*R,R*-tpadac)Tb][K]

Following general procedure, a white solid was obtained. ^{1}H NMR (D_2O, 400 MHz): δ (ppm): -54.46, -50.97, -45.17, -34.44, -26.29, 1.15, 13.32, 17.46, 24.60, 35.74, 49.94. Due to paramagnetism, integration of the spectrum is not accurate. All efforts to obtain ^{13}C NMR were unsuccessful. HRMS for $C_{34}H_{31}N_6TbO_8Na^+$ ([M−K+H+Na]$^+$), calculated 833.135, found 833.1327. Elemental Analysis [(*R,R*-tpadac)Tb][K]·3H_2O Calcd (%): C, 45.24; H, 4.02; N, 9.31. Found (%): C, 45.28; H, 4.09; N, 9.39.

Synthesis of [(*R,R*-tpadac)Eu][K]

Following general procedure, a white solid was obtained. ^{1}H NMR (D_2O, 400 MHz): δ (ppm): 0.75, 2.51, 3.03, 4.05, 5.24, 5.50, 6.23, 11.05. Due to paramagnetism, integration of the spectrum is not accurate. All efforts to obtain ^{13}C NMR were unsuccessful. HRMS for $C_{34}H_{31}N_6EuO_8Na^+$ ([M−K+H+Na]$^+$), calculated 827.131, found 827.1260; $C_{34}H_{32}N_6EuO_8^+$ ([M−K+2H]$^+$), calculated 805.149, found 805.1354. Elemental Analysis [(*R,R*-tpadac)Eu][K]·3H_2O Calcd (%): C, 45.59; H, 4.05; N, 9.38. Found (%): C, 45.51; H, 3.99; N, 9.30.

Synthesis of [(*R,R*-tpadac)Dy][K]

Following general procedure, a white solid was obtained. ^{1}H NMR (D_2O, 400 MHz): δ (ppm): -72.07, -53.79, -49.42, -43.03, -38.10, -28.87, 1.36, 9.91, 22.94, 44.52, 74.47. Due to paramagnetism, integration of the spectrum is not accurate. All efforts to obtain ^{13}C NMR were unsuccessful. HRMS for $C_{34}H_{31}N_6DyO_8K^+$ ([M+H]$^+$), calculated 854.113, found 854.1025; $C_{34}H_{32}N_6DyO_8^+$ ([M−K+2H]$^+$), calculated 816.157, found 816.1500. Elemental Analysis [(*R,R*-tpadac)Dy][K]·2H_2O Calcd (%): C, 45.97; H, 3.86; N, 9.46. Found (%): C, 46.01; H, 3.82; N, 9.41.

Synthesis of [(*R,R*-tpadac)Sm][K]

Following general procedure, a white solid was obtained. ^{1}H NMR (D_2O, 400 MHz): δ (ppm): 0.76 (br, 2H), 1.10 (br, 2H), 1.22 (br, 2H), 1.47 (br, 2H), 1.69 (br, 2H), 2.92 (d, *J* = 15.2 Hz, 2H), 3.68 (d, *J* = 17.5 Hz, 2H), 3.78 (d, *J* = 17.6 Hz, 2H), 3.99 (d, *J* = 15.1 Hz, 2H), 7.39 (d, *J* = 7.8 Hz, 2H), 7.63 (d, *J* = 7.7 Hz, 2H), 7.82 (d, *J* = 7.6 Hz, 2H), 8.00 (t, *J* = 7.7 Hz, 2H), 8.07 (d, *J* = 7.7 Hz, 2H), 8.20 (t, *J* = 7.8 Hz, 2H). HRMS for $C_{34}H_{31}N_6SmO_8Na^+$ ([M−K+H+Na]$^+$), calculated 826.130, found 826.1224. Elemental Analysis [(*R,R*-tpadac)Sm][K]·3H_2O Calcd (%): C, 45.67; H, 4.06; N, 9.40. Found (%): C, 45.62; H, 4.04; N, 9.42.

Synthesis of [(*S,S*-tpadac)La][K]

Following general procedure, a white solid was obtained. ^{1}H NMR (D_2O, 400 MHz): δ (ppm): 1.02 (br, 2H), 1.55 (br, 2H), 1.75 (br, 2H), 2.02 (br, 2H), 2.32 (br, 2H), 3.05 (d, *J* = 15.8 Hz, 2H), 3.51 (d, *J* = 16.2 Hz, 2H), 3.96 (d, *J* = 15.9 Hz, 2H), 4.06 (d, *J* = 15.9 Hz, 2H), 7.35 (d, *J* = 7.7 Hz, 2H), 7.39 (d, *J* = 7.7 Hz, 2H), 7.70 (d, *J* = 7.7 Hz, 2H), 7.90 (dt, *J* = 12.6, 7.9 Hz, 4H), 7.95 (dd, *J* = 9.5, 5.9 Hz, 2H). ^{13}C NMR (D_2O, 400 MHz): δ (ppm): 24.04, 24.30, 53.57, 59.89, 66.03, 123.29, 123.58, 124.85, 126.26, 140.45, 141.57, 151.02, 152.02, 155.11, 159.35, 171.14, 172.98. HRMS for $C_{34}H_{31}N_6LaO_8K^+$ ([M+H]$^+$), calculated 829.090, found 829.0772; $C_{34}H_{32}N_6LaO_8^+$ ([M−K+2H]$^+$), calculated 791.135, found 791.1022. Elemental Analysis [(*S,S*-tpadac)La][K]·4H_2O Calcd (%): C, 45.34; H, 4.25; N, 9.33. Found (%): C, 45.28; H, 4.19; N, 9.24.

Synthesis of [(*S,S*-tpadac)Tb][K]

Following general procedure, a white solid was obtained. ^{1}H NMR (D_2O, 400 MHz): δ (ppm): -49.60, -47.87, -42.89, -33.00, -25.10, 1.17, 13.47, 14.33, 28.40, 37.55, 49.70. Due to paramagnetism, integration of the spectrum is not accurate. HRMS for $C_{34}H_{31}N_6TbO_8K^+$ ([M+H]$^+$), calculated 849.109, found 849.0905; $C_{34}H_{32}N_6TbO_8^+$ ([M−K+2H]$^+$), calculated 811.154, found 811.1334. Elemental Analysis [(*S,S*-tpadac)Tb][K]·3H_2O Calcd (%): C, 45.24; H, 4.02; N, 9.31. Found (%): C, 45.17; H, 4.09; N, 9.26.

Synthesis of [(*S*,*S*-tpadac)Eu][K]

Following general procedure, a white solid was obtained. ^{1}H NMR (D_2O, 400 MHz): δ (ppm): 0.76, 1.87, 2.52, 3.02, 3.88, 5.43, 6.19, 11.24. Due to paramagnetism, integration of the spectrum is not accurate. HRMS for $C_{34}H_{31}N_6EuO_8K^+$ ($[M+H]^+$), calculated 843.105, found 843.0886; $C_{34}H_{32}N_6EuO_8^+$ ($[M-K+2H]^+$), calculated 805.149, found 805.1463. Elemental Analysis [(*S*,*S*-tpadac)Eu][K]·3H_2O Calcd (%): C, 45.59; H, 4.05; N, 9.38. Found (%): C, 45.51; H, 3.99; N, 9.30.

Synthesis of [(*S*,*S*-tpadac)Dy][K]

Following general procedure, a white solid was obtained. ^{1}H NMR (D_2O, 400 MHz): δ (ppm): -73.41, -55.52, -50.57, -39.72, -30.25, 1.42, 12.13, 21.33, 40.68, 70.52. Due to paramagnetism, integration of the spectrum is not accurate. HRMS for $C_{34}H_{31}N_6DyO_8K^+$ ($[M+H]^+$), calculated 854.113, found 854.0902; $C_{34}H_{32}N_6DyO_8^+$ ($[M-K+2H]^+$), calculated 816.157, found 816.1391. Elemental Analysis [(*S*,*S*-tpadac)Dy][K]·2H_2O Calcd (%): C, 45.97; H, 3.86; N, 9.46. Found (%): C, 46.05; H, 3.81; N, 9.41.

Synthesis of [(*S*,*S*-tpadac)Sm][K]

Following general procedure, a white solid was obtained. ^{1}H NMR (D_2O, 400 MHz): δ (ppm): 0.76 (br, 2H), 1.12 (br, 2H), 1.23 (br, 2H), 1.50 (br, 2H), 1.69 (br, 2H), 2.89 (d, *J* = 15.3 Hz, 2H), 3.67 (d, *J* = 17.5 Hz, 4H), 3.73 (d, *J* = 17.4 Hz, 2H), 3.97 (d, *J* = 15.3 Hz, 2H), 7.39 (d, *J* = 7.8 Hz, 2H), 7.60 (d, *J* = 7.7 Hz, 2H), 7.81 (d, *J* = 7.7 Hz, 2H), 7.98 (t, *J* = 7.7 Hz, 2H), 8.07 (d, *J* = 7.7 Hz, 2H), 8.17 (t, *J* = 7.7 Hz, 2H). HRMS for $C_{34}H_{31}N_6SmO_8K^+$ ($[M+H]^+$), calculated 842.104, found 842.0911; $C_{34}H_{32}N_6SmO_8^+$ ($[M-K+2H]^+$), calculated 804.148, found 804.1384. Elemental Analysis [(*S*,*S*-tpadac)Sm][K]·3H_2O Calcd (%): C, 45.67; H, 4.06; N, 9.40. Found (%): C, 45.70; H, 4.02; N, 9.46.

NMR Spectra of [(*S*,*S*-tpadac)La][K]

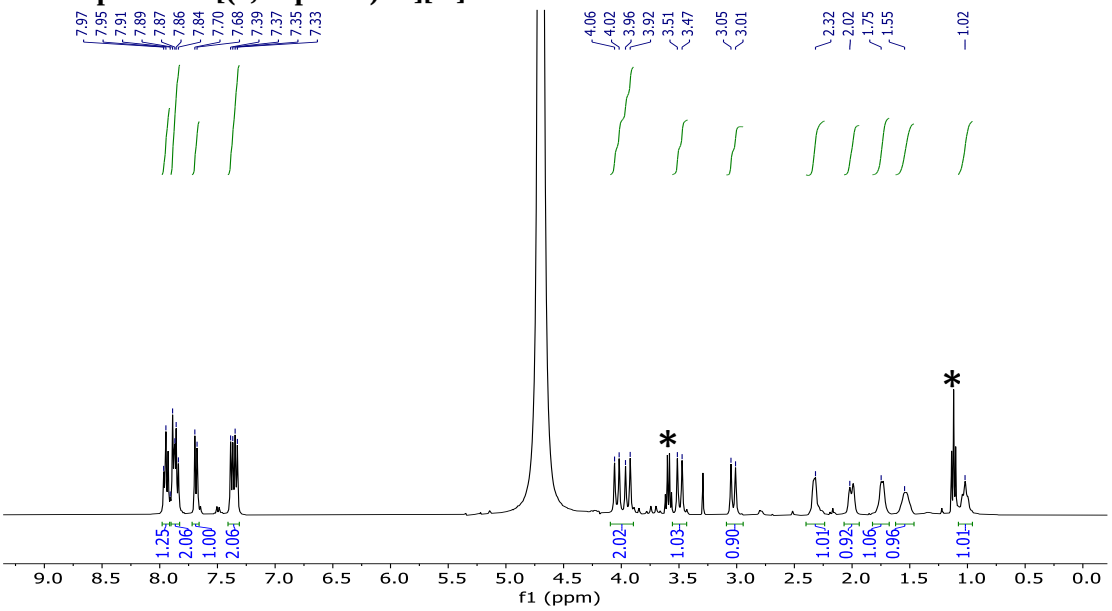

* = ethanol

Figure S1: ^{1}H NMR of [(*S*,*S*-tpadac)La][K] in D_2O at 298 K

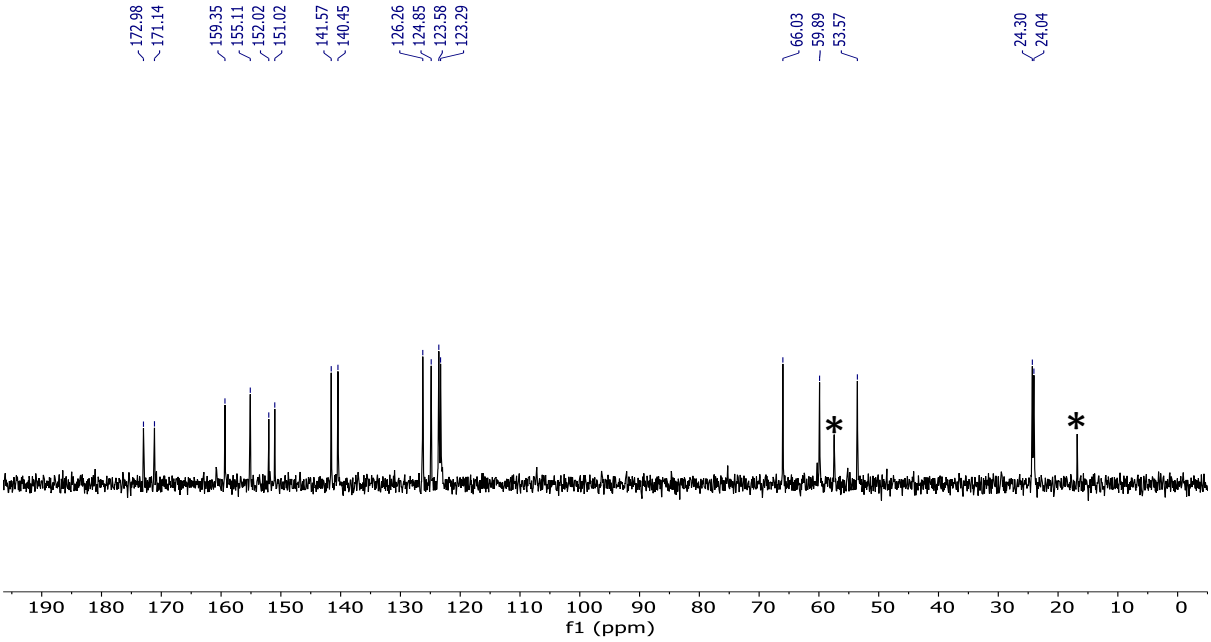

* = ethanol

Figure S2: ^{13}C NMR of [(*S*,*S*-tpadac)La][K] in D_2O at 298 K

^{1}H NMR Spectra of [(*R*,*R*-tpadac)Sm][K] and [(*S*,*S*-tpadac)Sm][K]

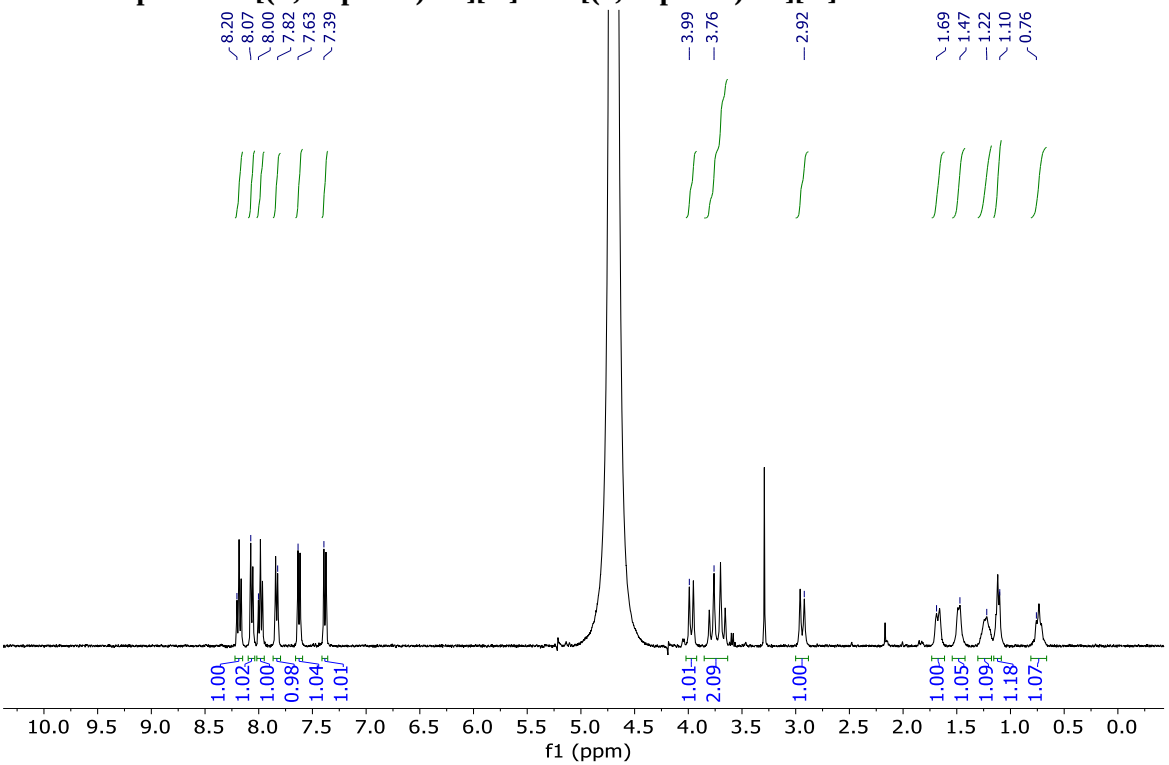

Figure S3: ^{1}H NMR of [(*R*,*R*-tpadac)Sm][K] in D_2O at 298 K

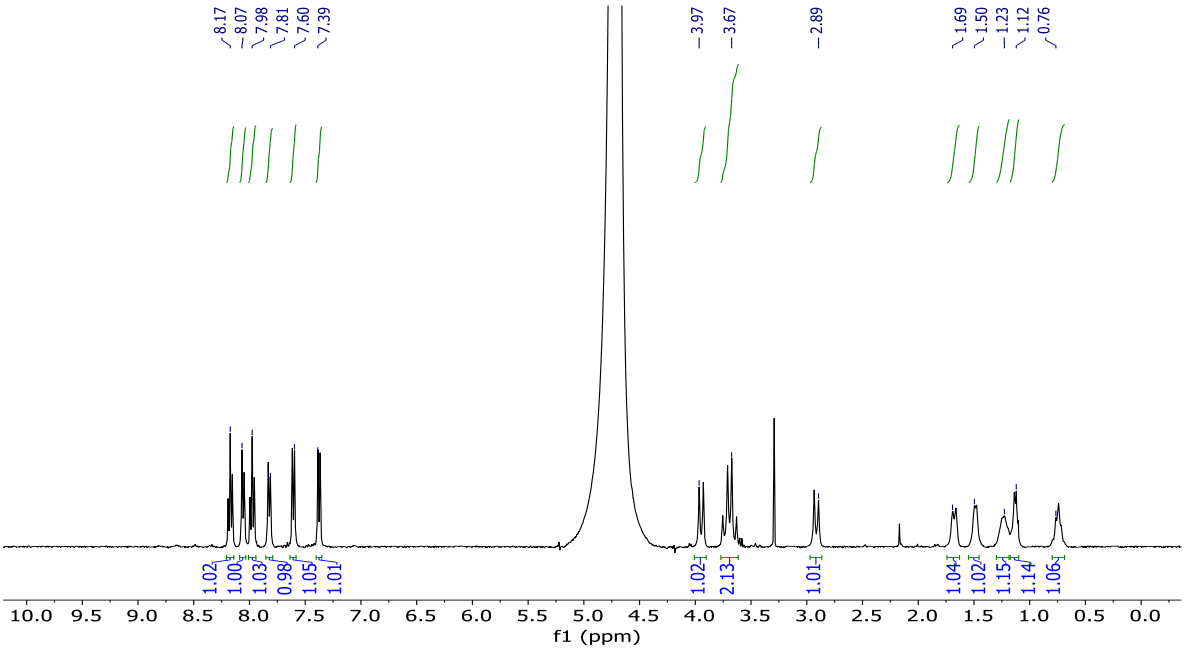

Figure S4: ^{1}H NMR of [(*S*,*S*-tpadac)Sm][K] in D_2O at 298 K

^{1}H NMR Spectra of [(*R*,*R*-tpadac)Eu][K] and [(*S*,*S*-tpadac)Eu][K]

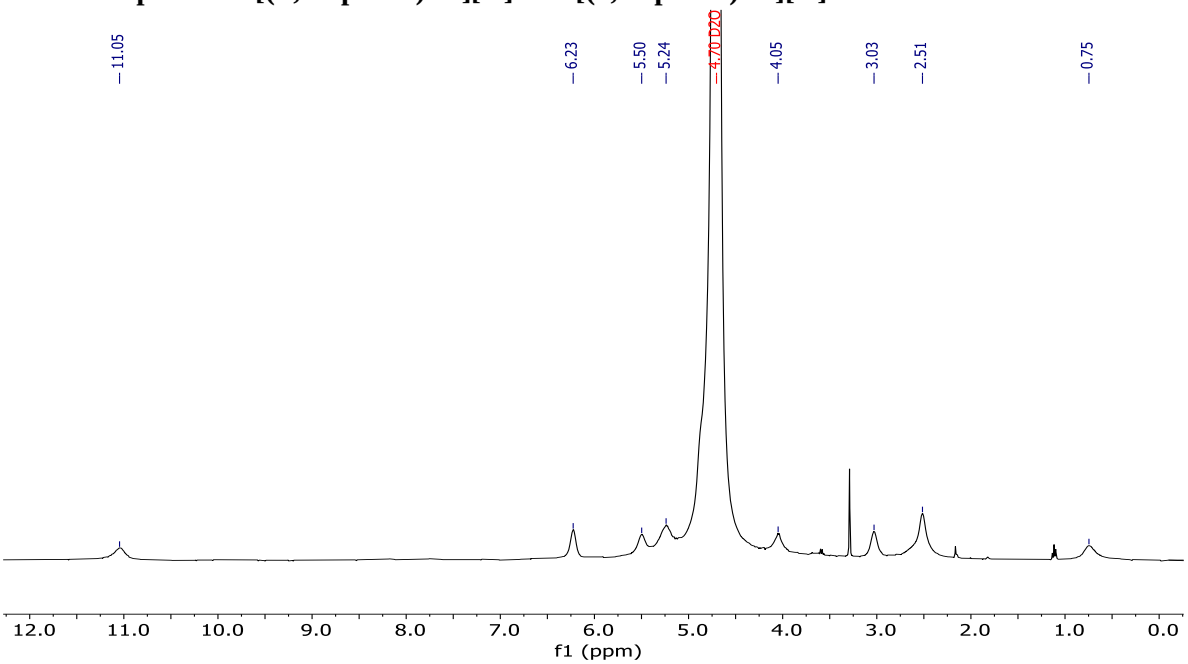

Figure S5: ^{1}H NMR of [(*R*,*R*-tpadac)Eu][K] in D_2O at 298 K

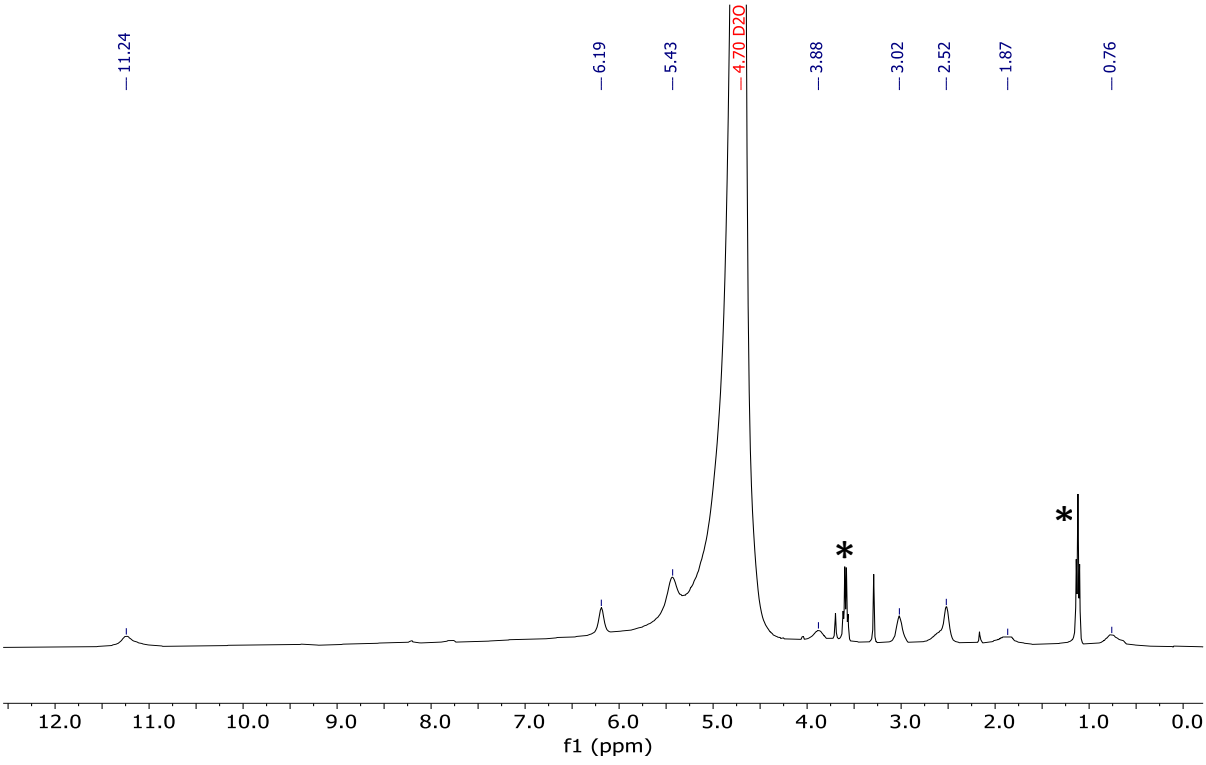

* = ethanol

Figure S6: ^{1}H NMR of [(*S*,*S*-tpadac)Eu][K] in D_2O at 298 K

^{1}H NMR Spectra of [(*R*,*R*-tpadac)Tb][K] and [(*S*,*S*-tpadac)Tb][K]

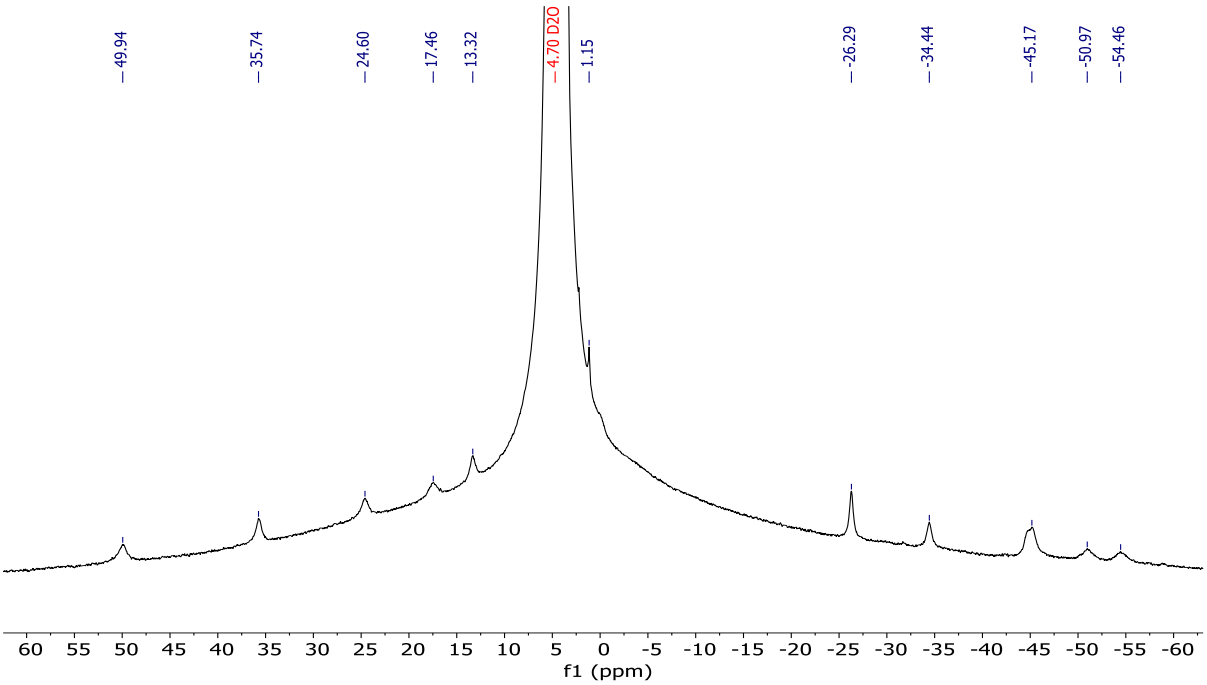

Figure S7: ^{1}H NMR of [(*R*,*R*-tpadac)Tb][K] in D_2O at 298 K

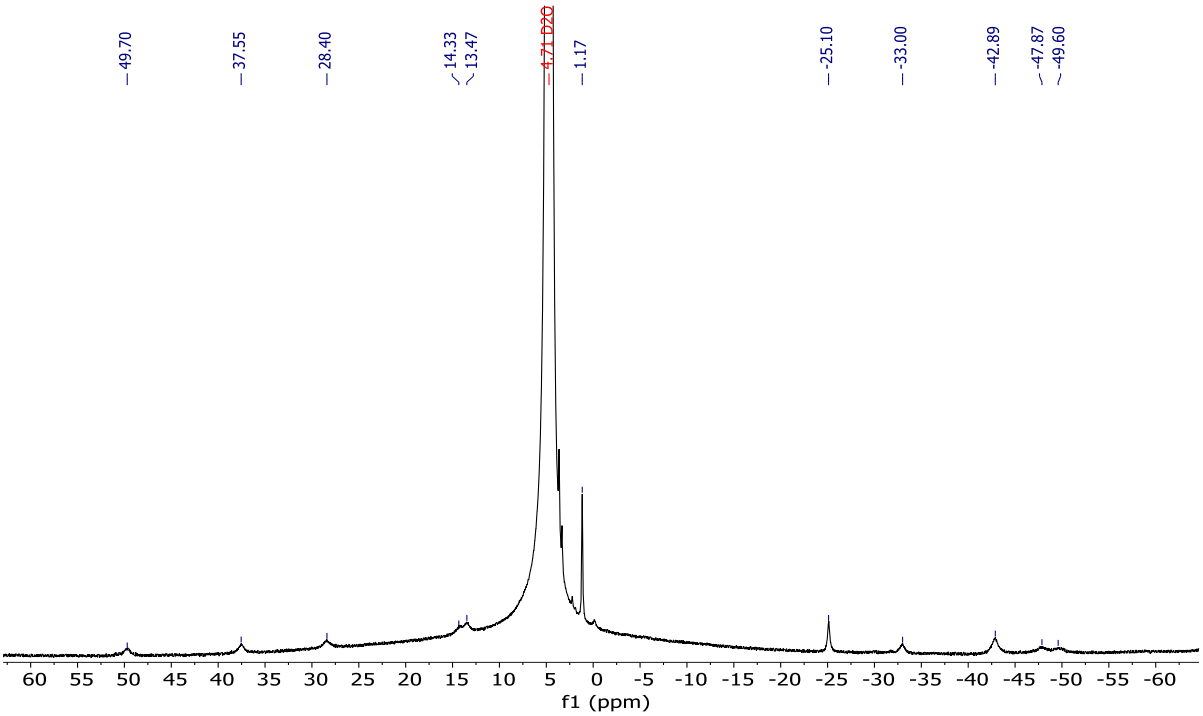

Figure S8: ^{1}H NMR of [(*S*,*S*-tpadac)Tb][K] in D_2O at 298 K

^{1}H NMR Spectra of [(*R*,*R*-tpadac)Dy][K] and [(*S*,*S*-tpadac)Dy][K]

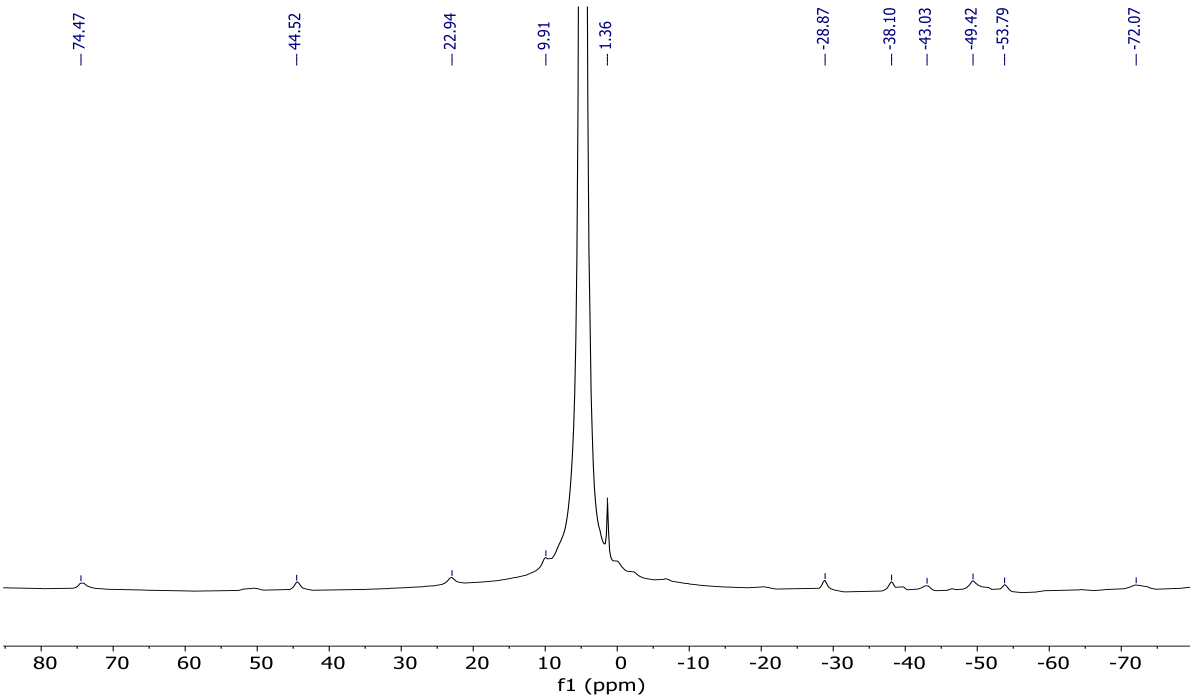

Figure S9: ^{1}H NMR of [(*R*,*R*-tpadac)Dy][K] in D_2O at 298 K

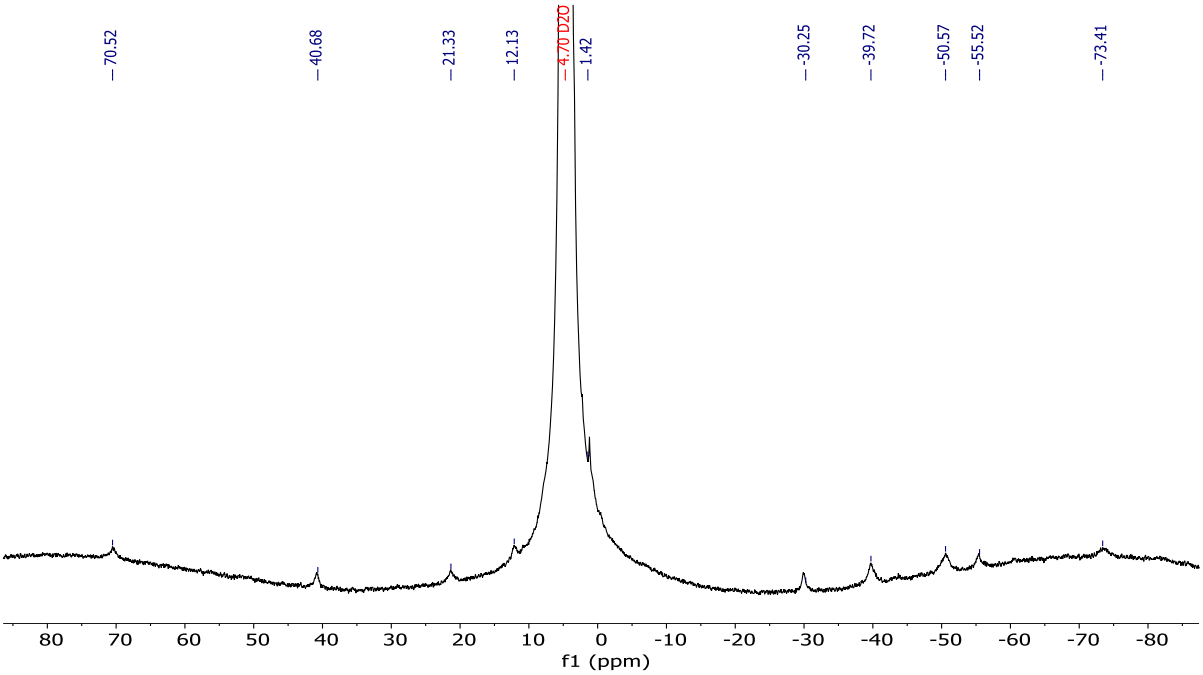

Figure S10: ^{1}H NMR of [(*S*,*S*-tpadac)Dy][K] in D_2O at 298 K

UV/Visible Absorbance/Emission Spectra

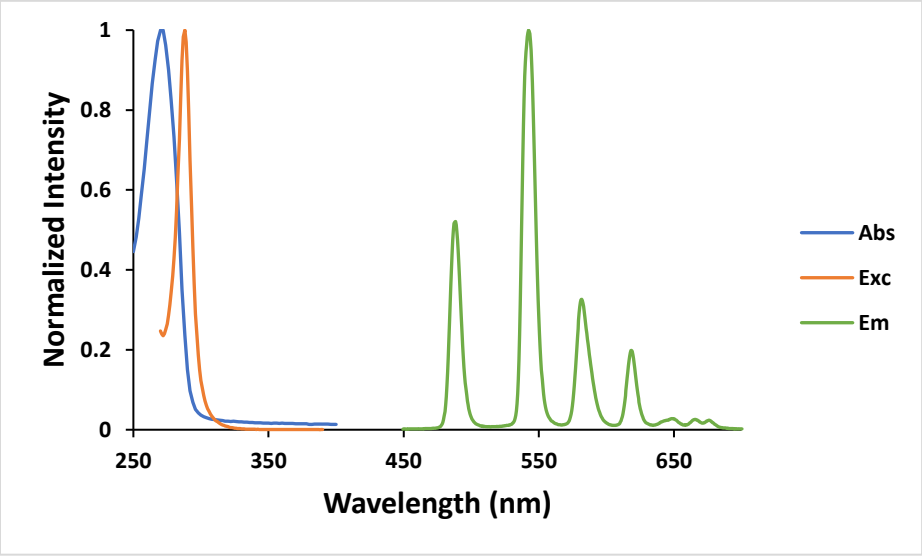

Figure S11: Normalized UV-visible absorbance (blue), excitation (orange), and emission (green) spectra of $[(S,S\text{-tpadac})Tb]^-_{(aq)}[K]^+_{(aq)}$ (6.13×10^{-4} M for emission and 2.36×10^{-5} M for absorbance) in 0.1 M tris buffer (pH 7.4) at room temperature. Excitation at 290 nm. Bandpass: 5 nm. Identical spectrum was observed for the (*R*,*R*)- enantiomer.

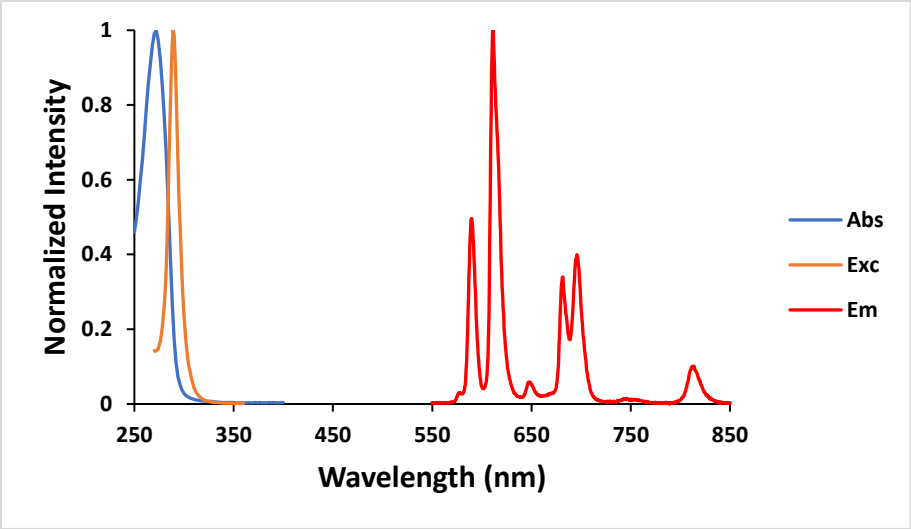

Figure S12: Normalized UV-visible absorbance (blue), excitation (orange), and emission (red) spectra of $[(S,S\text{-tpadac})Eu]^-_{(aq)}[K]^+_{(aq)}$ (6.1×10^{-4} M for emission and 3.0×10^{-5} M for absorbance) in 0.1 M tris buffer (pH 7.4) at room temperature. Excitation at 290 nm. Bandpass: 5 nm. Identical spectrum was observed for the (*R*,*R*)- enantiomer.

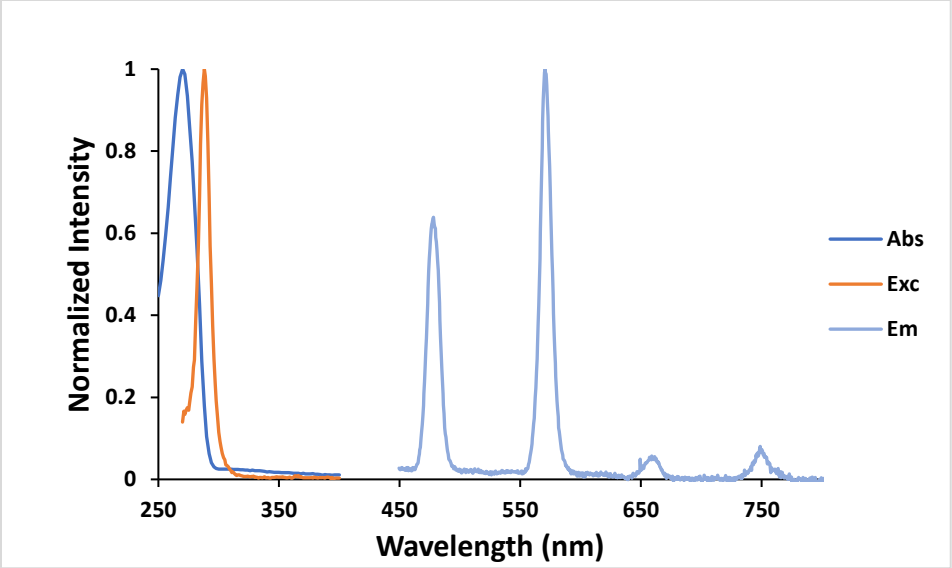

Figure S13: Normalized UV-visible absorbance (blue), excitation (orange), and emission (teal) spectra of $[(S,S\text{-tpadac})Dy]^-_{(aq)}[K]^+_{(aq)}$ (6.1 x 10^{-4} M for emission and 3.0 x 10^{-5} M for absorbance) in 0.1 M tris buffer (pH 7.4) at room temperature. Excitation at 290 nm. Bandpass: 5 nm. Identical spectrum was observed for the (R,R)- enantiomer.

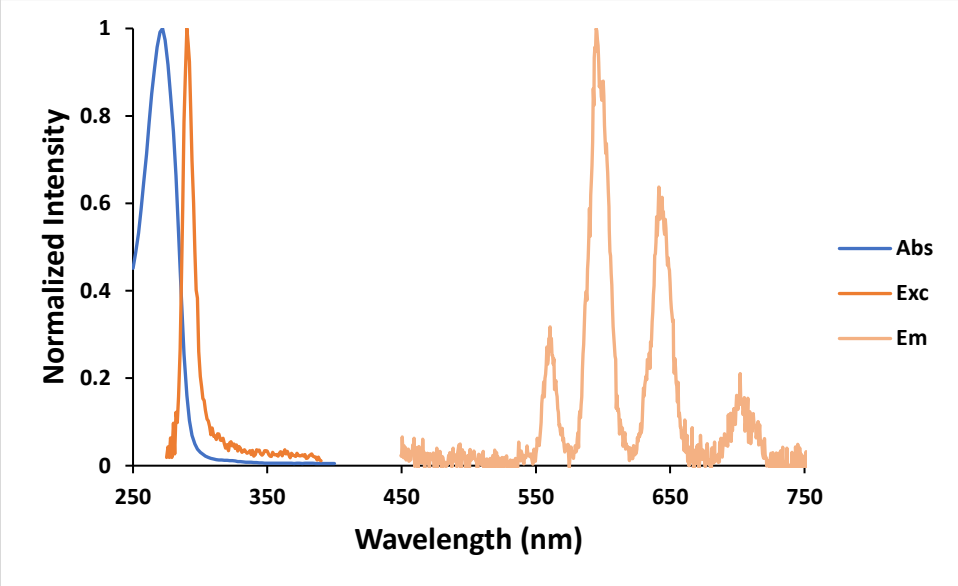

Figure S14: Normalized UV-visible absorbance (blue), excitation (orange), and emission (apricot) spectra of $[(S,S\text{-tpadac})Sm]^-_{(aq)}[K]^+_{(aq)}$ (6.1 x 10^{-4} M for emission and 3.0 x 10^{-5} M for absorbance) in 0.1 M tris buffer (pH 7.4) at room temperature. Excitation at 290 nm. Bandpass: 5 nm. Identical spectrum was observed for the (*R*,*R*)- enantiomer.

Circularly Polarized Luminescence Spectra

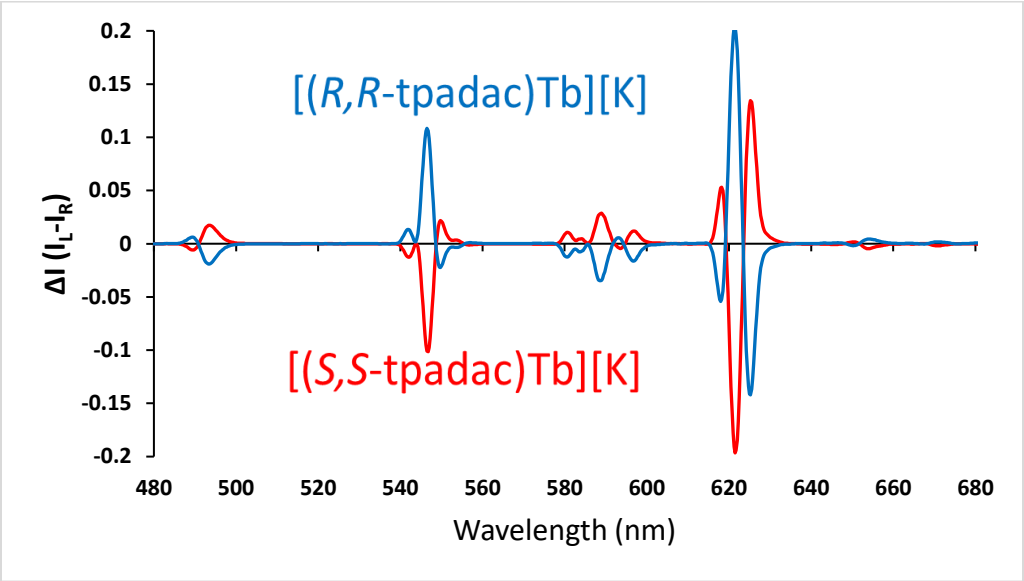

Figure S15: Normalized Δ*I* Spectra of $[(R,R\text{-tpadac})Tb]^{-}_{(aq)}[K]^{+}_{(aq)}$ and $[(S,S\text{-tpadac})Tb]^{-}_{(aq)}[K]^{+}_{(aq)}$. Concentration is 6.1 x 10^{-4} M in 0.1 M tris buffer, pH 7.4. 295 nm excitation LED. Slit width 2.4 nm. Average of 60 scans, 12 minutes per scan.

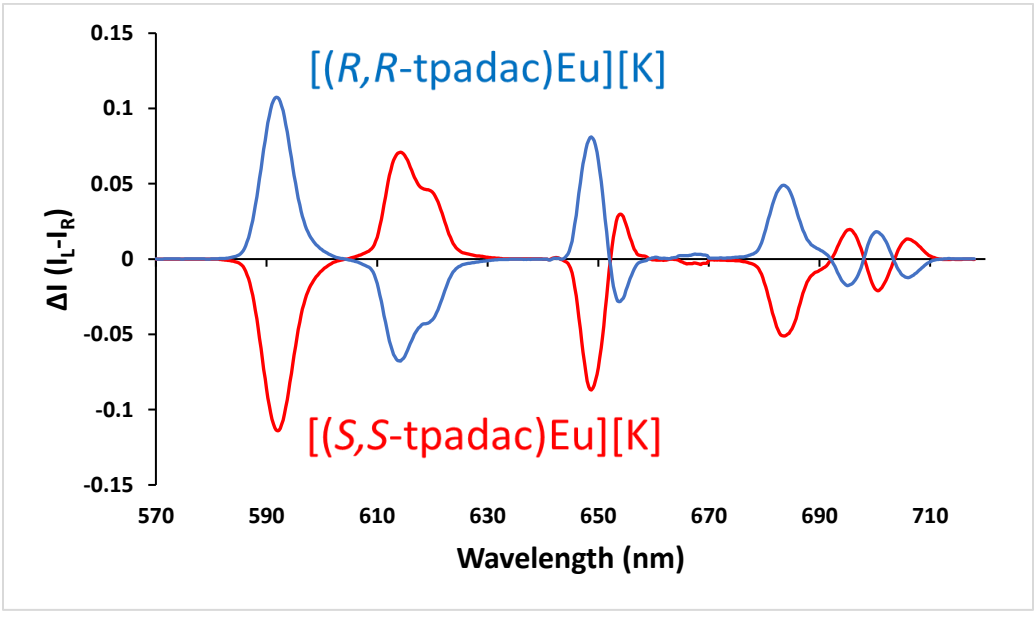

Figure S16: Normalized Δ*I* Spectra of $[(R,R\text{-tpadac})Eu]^{-}_{(aq)}[K]^{+}_{(aq)}$ and $[(S,S\text{-tpadac})Eu]^{-}_{(aq)}[K]^{+}_{(aq)}$. Concentration is 6.1 x 10^{-4} M in 0.1 M tris buffer, pH 7.4. 295 nm excitation LED. Slit width 5 nm. Average of 87 scans, 10 minutes per scan

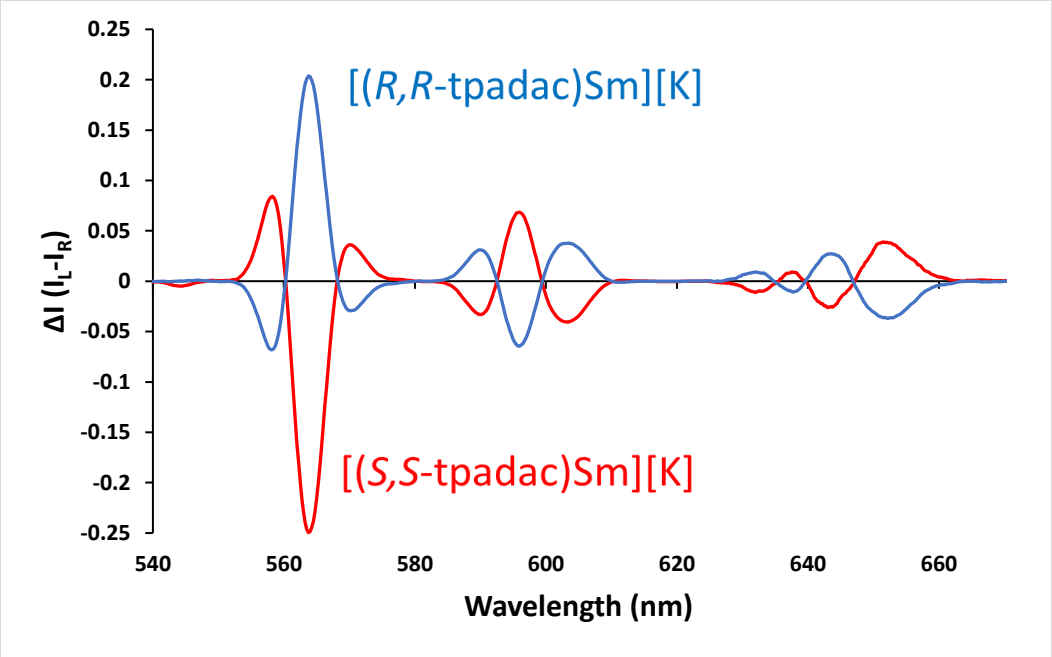

Figure S17: Normalized Δ*I* Spectra of [(*R*,*R*-tpadac)Sm]$^{-}_{(aq)}$[K]$^{+}_{(aq)}$ and [(*S*,*S*-tpadac)Sm]$^{-}_{(aq)}$[K]$^{+}_{(aq)}$. Concentration is 6.1 x 10^{-4} M in 0.1 M tris buffer, pH 7.4. 295 nm excitation LED. Slit width 5 nm. Average of 48 scans, 9 minutes per scan.

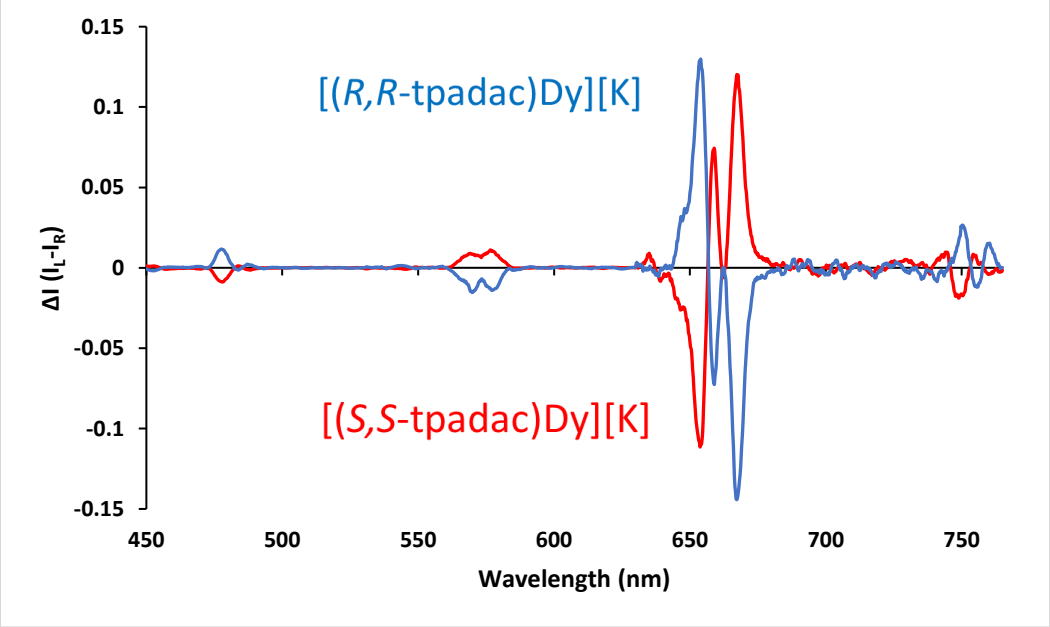

Figure S18: Normalized Δ*I* Spectra of [(*R*,*R*-tpadac)Dy]$^{-}_{(aq)}$[K]$^{+}_{(aq)}$ and [(*S*,*S*-tpadac)Dy]$^{-}_{(aq)}$[K]$^{+}_{(aq)}$. Concentration is 6.1 x 10^{-4} M in 0.1 M tris buffer, pH 7.4. 295 nm excitation LED. Slit width 5 nm. Average of 31 scans, 20 minutes per scan.

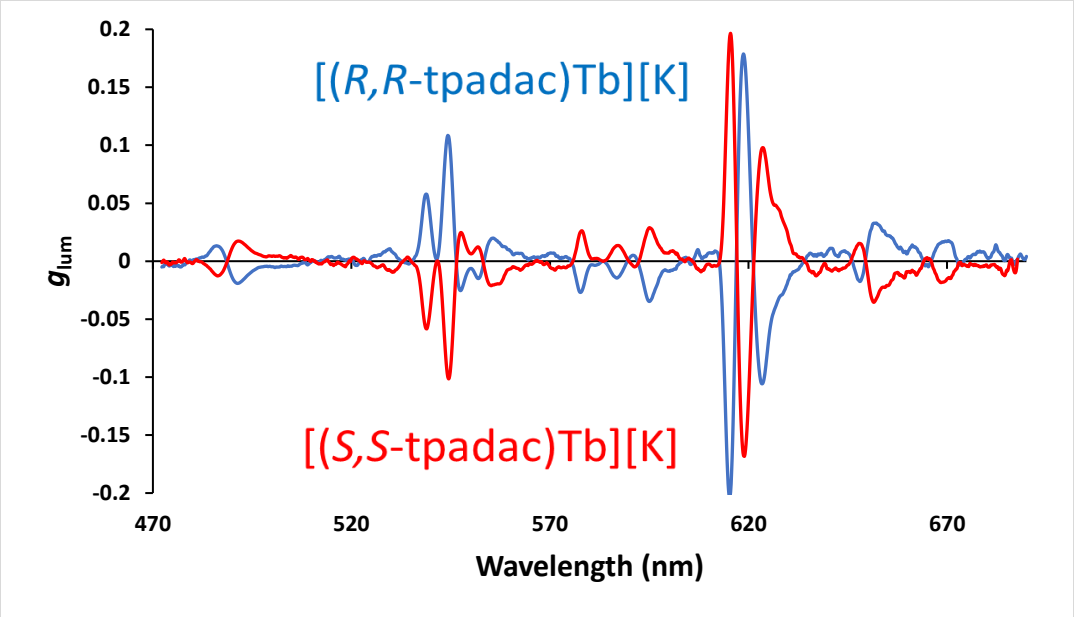

Figure S19: Circularly Polarized Luminescence Spectra of $[(R,R\text{-tpadac})Tb]^-_{(aq)}[K]^+_{(aq)}$ and $[(S,S\text{-tpadac})Tb]^-_{(aq)}[K]^+_{(aq)}$. Concentration is 6.1 x 10^{-4} M in 0.1 M tris buffer, pH 7.4. 295 nm excitation LED. Slit width 2.4 nm. Average of 60 scans, 12 minutes per scan.

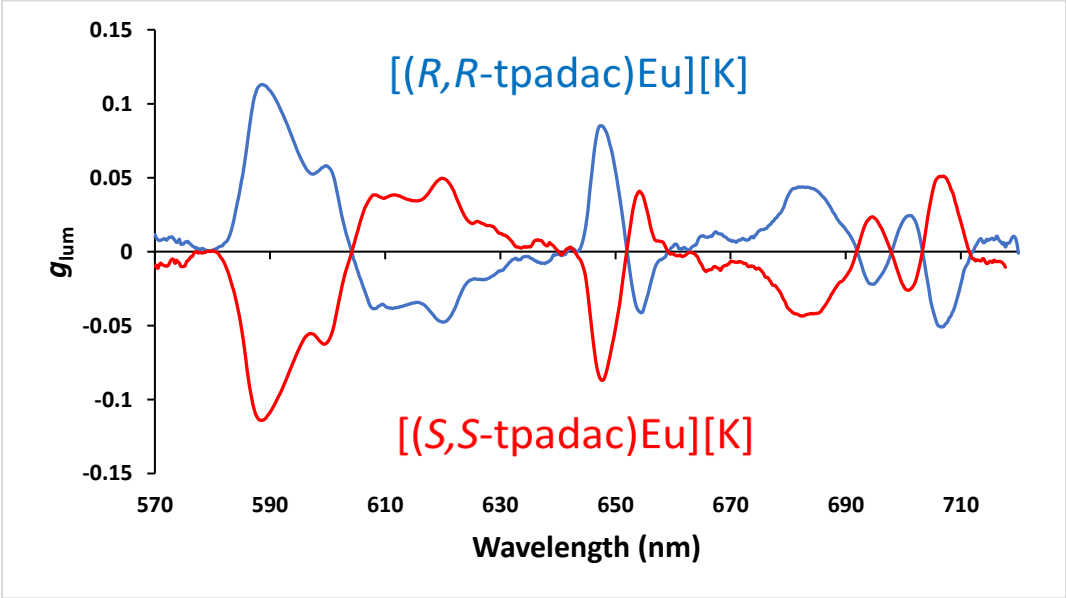

Figure S20: Circularly Polarized Luminescence Spectra of $[(R,R\text{-tpadac})Eu]^-_{(aq)}[K]^+_{(aq)}$ and $[(S,S\text{-tpadac})Eu]^-_{(aq)}[K]^+_{(aq)}$. Concentration is 6.1 x 10^{-4} M in 0.1 M tris buffer, pH 7.4. 295 nm excitation LED. Slit width 5 nm. Average of 87 scans, 10 minutes per scan.

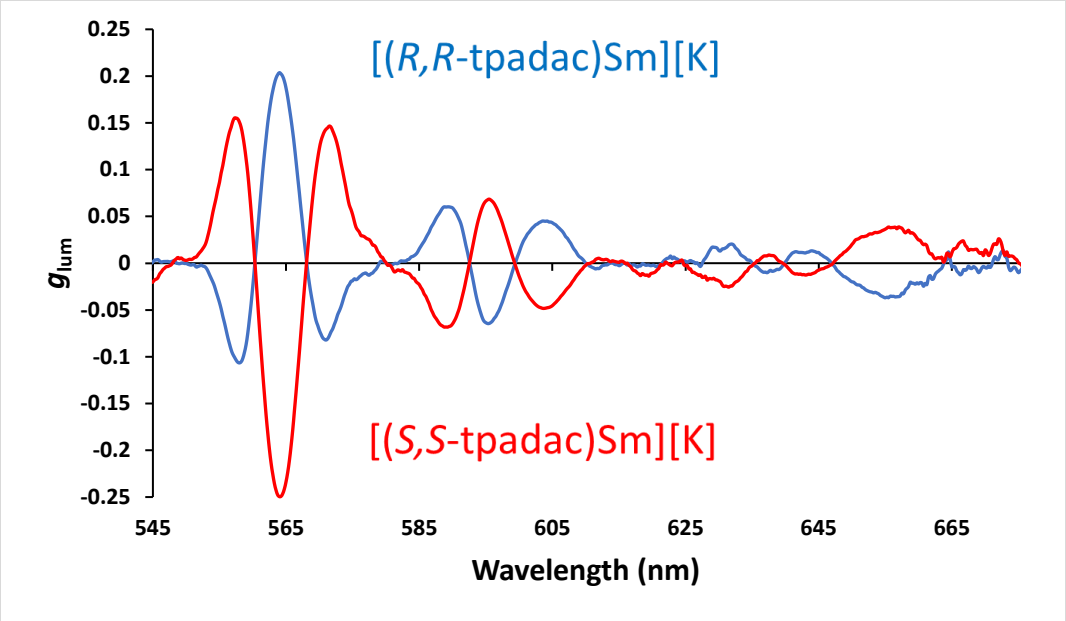

Figure S21: Circularly Polarized Luminescence Spectra of $[(R,R\text{-tpadac})Sm]^{-}_{(aq)}[K]^{+}_{(aq)}$ and $[(S,S\text{-tpadac})Sm]^{-}_{(aq)}[K]^{+}_{(aq)}$. Concentration is 6.1 x 10^{-4} M in 0.1 M tris buffer, pH 7.4. 295 nm excitation LED. Slit width 5 nm. Average of 48 scans, 9 minutes per scan.

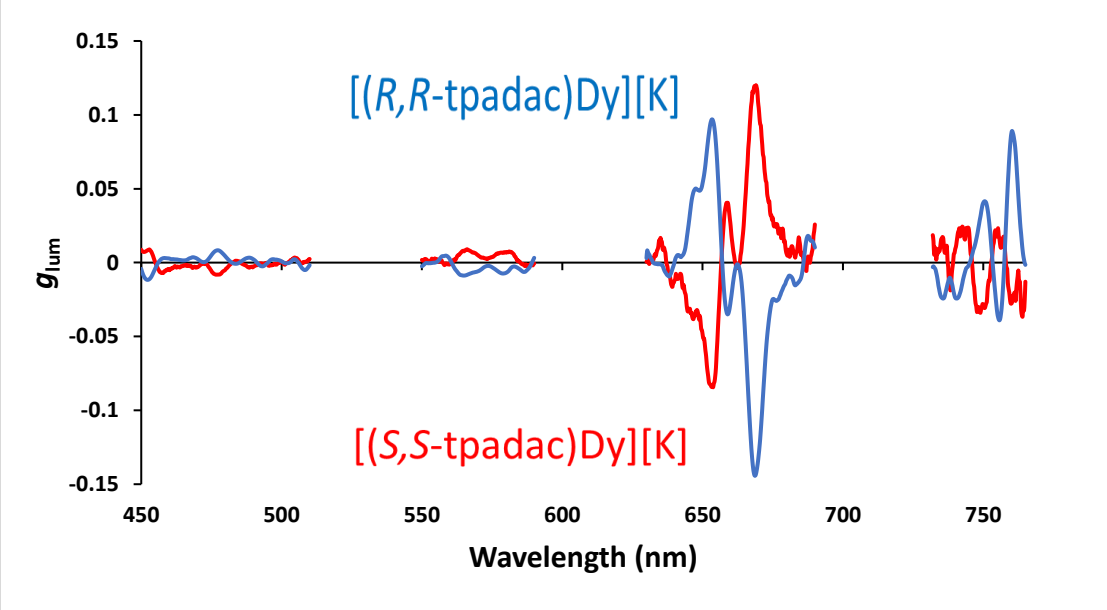

Figure S22: Circularly Polarized Luminescence Spectra of $[(R,R\text{-tpadac})Dy]^{-}_{(aq)}[K]^{+}_{(aq)}$ and $[(S,S\text{-tpadac})Dy]^{-}_{(aq)}[K]^{+}_{(aq)}$. Concentration is 6.1 x 10^{-4} M in 0.1 M tris buffer, pH 7.4. 295 nm excitation LED. Slit width 5 nm. Average of 31 scans, 20 minutes per scan**.**

CPL Brightness

Table S1: Tabulated CPL Brightness Data

[(tpadac)Ln][K]	Φ	ε ($M^{-1}cm^{-1}$)	Transition	λ (nm)	g_{lum}	β_i	B_{CPL} ($M^{-1}cm^{-1}$)
Tb	0.47	20500	$^5D_4 \rightarrow {}^7F_6$	491	0.02	0.21	20.23
			$^5D_4 \rightarrow {}^7F_5$	544	0.11	0.48	245.4
			$^5D_4 \rightarrow {}^7F_4$	594	0.03	0.17	24.57
			$^5D_4 \rightarrow {}^7F_3$	618	0.20	0.08	77.08
Eu	0.065	19300	$^5D_0 \rightarrow {}^7F_0$	-	Negligible	Negligible	Negligible
			$^5D_0 \rightarrow {}^7F_1$	589	0.11	0.16	11.04
			$^5D_0 \rightarrow {}^7F_2$	620	0.05	0.40	12.55
			$^5D_0 \rightarrow {}^7F_3$	649	0.08	0.01	0.502
			$^5D_0 \rightarrow {}^7F_4$	684	0.04	0.12	3.011
			$^5D_0 \rightarrow {}^7F_5$	707	0.05	0.19	5.959
Dy	0.0144	16900	$^4F_{9/2} \rightarrow {}^6H_{15/2}$	478	0.01	0.35	0.426
			$^4F_{9/2} \rightarrow {}^6H_{13/2}$	572	0.01	0.50	0.608
			$^4F_{9/2} \rightarrow {}^6H_{11/2}$	668	0.14	0.04	0.681
			$^4F_{9/2} \rightarrow {}^6H_{9/2}$	750	0.03	0.05	0.183
Sm	0.0022	16600	$^4G_{5/2} \rightarrow {}^6H_{5/2}$	564	0.25	0.09	0.411
			$^4G_{5/2} \rightarrow {}^6H_{7/2}$	589	0.07	0.47	0.601
			$^4G_{5/2} \rightarrow {}^6H_{9/2}$	656	0.04	0.32	0.233
			$^4G_{5/2} \rightarrow {}^6H_{11/2}$	-	Negligible	0.09	Negligible

B_{CPL} values are calculated according to the equation: $B_{CPL} = ½ \times \varepsilon \times \Phi \times \beta_i \times |g_{lum}|$. Excitation wavelength is 295 nm.

pH Titration

pH Titration Procedure: To a 6.13 x 10^{-5} M solution of $[(S,S\text{-tpadac})Tb]^{-}_{(aq)}[K]^{+}_{(aq)}$ in 0.1 M tris buffer (pH 8.0) was 1 M HCl added in incremental amounts with the aid of a microsyringe until pH 6.0. Aliquot was taken for CPL measurement after each HCl addition as the pH was gradually reduced from 8.0 to 6.0. The same procedure was performed for $[(S,S\text{-tpadac})Eu]^{-}_{(aq)}[K]^{+}_{(aq)}$ also. The ΔI plot is not corrected for concentration. Each CPL measurement is an average of 15 scans for both pH and metal titrations, 4 minutes per scan.

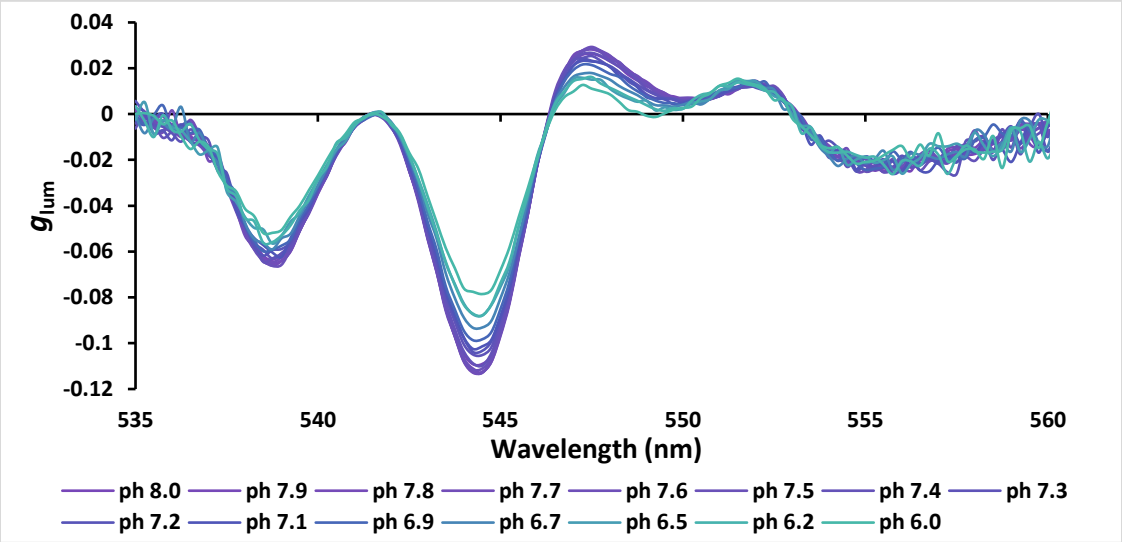

Figure S23: g_{lum} plot for pH titration of $[(S,S\text{-tpadac})Tb]^{-}_{(aq)}[K]^{+}_{(aq)}$ (6.13 x 10^{-5} M in 0.1 M tris buffer) against 1.0 M HCl for $^5D_4 \rightarrow {}^7F_5$ transition of Tb. 295 nm excitation LED. Slit width 2.4 nm.

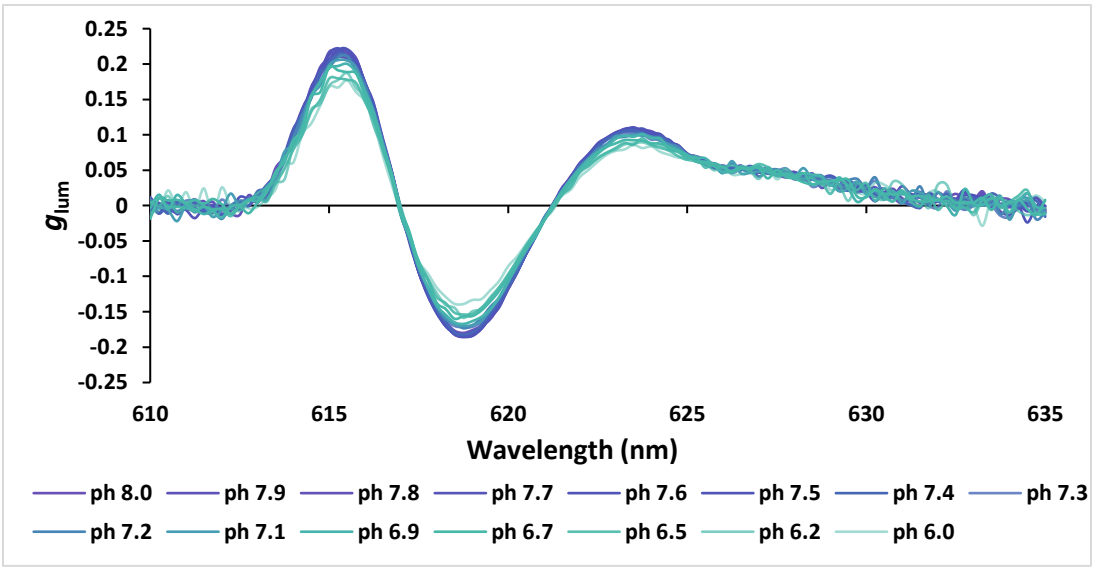

Figure S24: g_{lum} plot for pH titration of $[(S,S\text{-tpadac})Tb]^{-}_{(aq)}[K]^{+}_{(aq)}$ (6.13 x 10^{-5} M in 0.1 M tris buffer) against 1.0 M HCl for $^5D_4 \rightarrow {}^7F_3$ transition of Tb. 295 nm excitation LED. Slit width 2.4 nm.

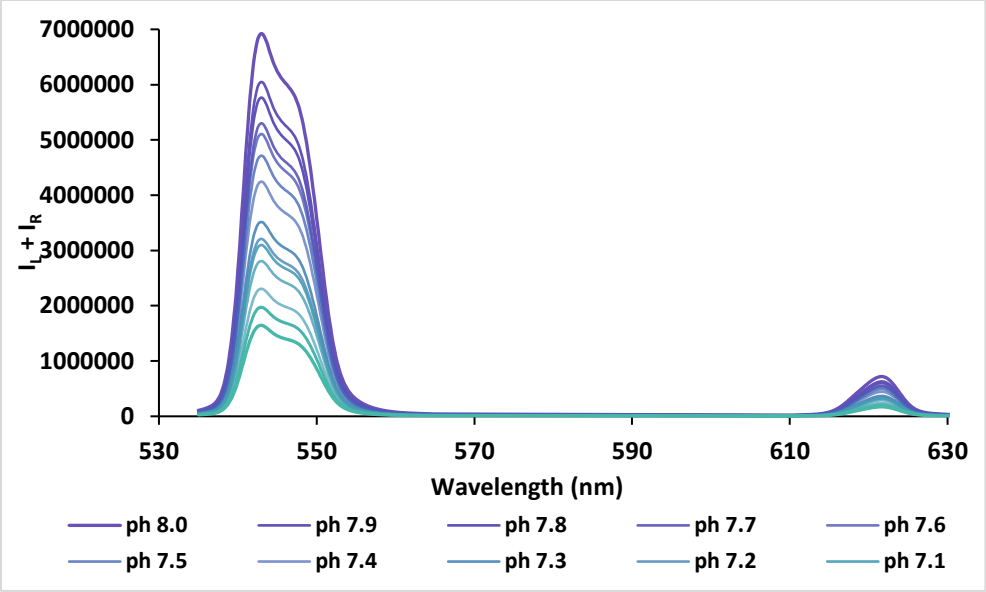

Figure S25: Total emission intensity plot for pH titration of $[(S,S\text{-tpadac})Tb]^-_{(aq)}[K]^+_{(aq)}$ (6.13×10^{-5} M in 0.1 M tris buffer) against 1.0 M HCl for $^5D_4 \rightarrow {}^7F_5$ and $^5D_4 \rightarrow {}^7F_3$ transitions of Tb. 295 nm excitation LED. Slit width 2.4 nm.

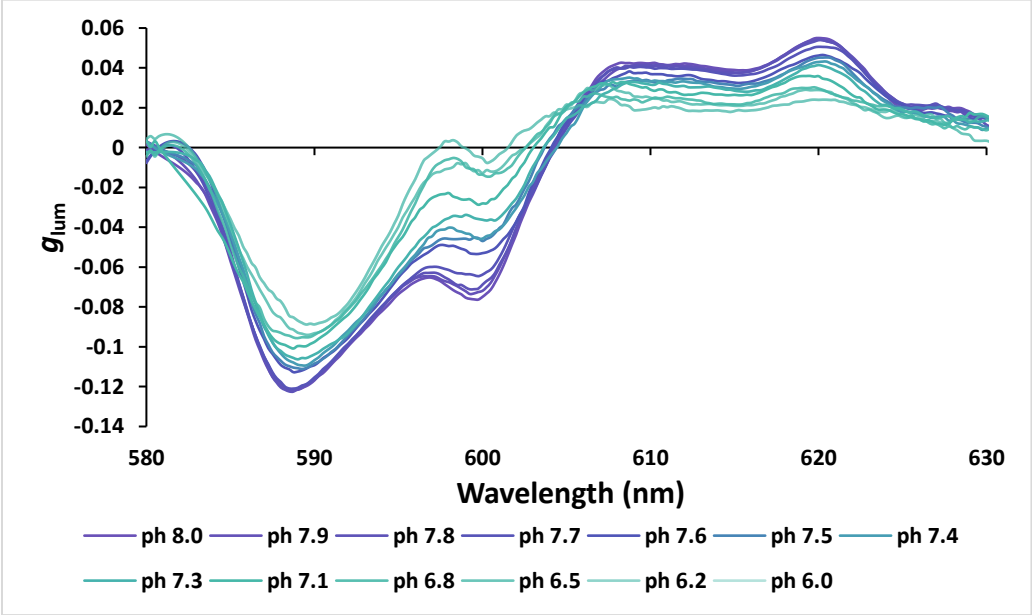

Figure S26: g_{lum} plot for pH titration of $[(S,S\text{-tpadac})Eu]^-_{(aq)}[K]^+_{(aq)}$ (6.1×10^{-5} M in 0.1 M tris buffer) against 1.0 M HCl for $^5D_0 \rightarrow {}^7F_1$ and $^5D_0 \rightarrow {}^7F_2$ transitions of Eu. 295 nm excitation LED lamp. Slit width 5 nm.

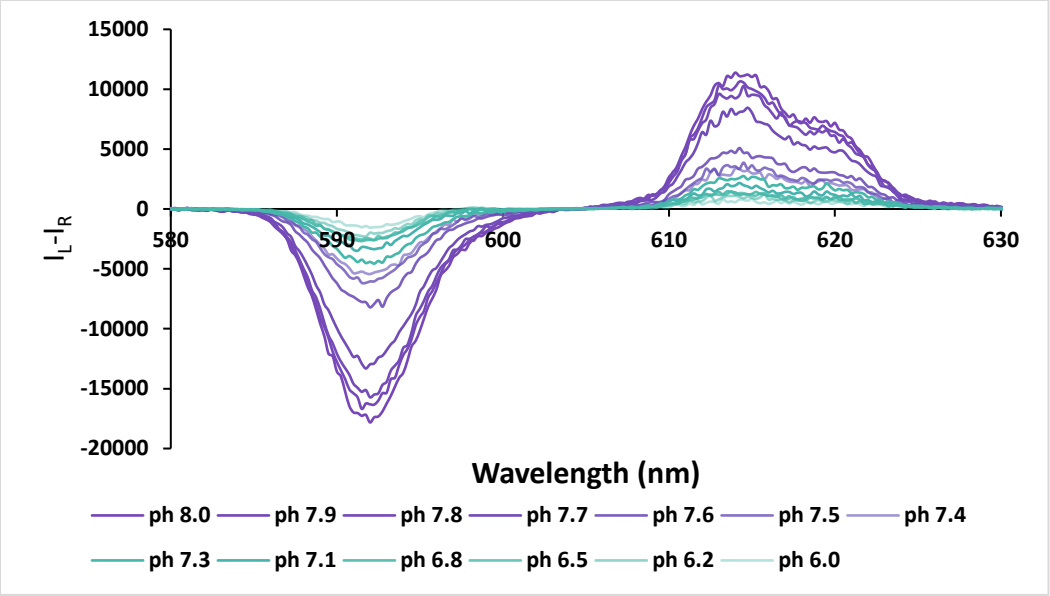

Figure S27: ΔI plot for pH titration of $[(S,S\text{-tpadac})Eu]^-_{(aq)}[K]^+_{(aq)}$ (6.13 x 10^{-5} M in 0.1 M tris buffer) against 1.0 M HCl for $^5D_0 \rightarrow {}^7F_1$ and $^5D_0 \rightarrow {}^7F_2$ transitions of Eu. 295 nm excitation LED. Slit width 5 nm.

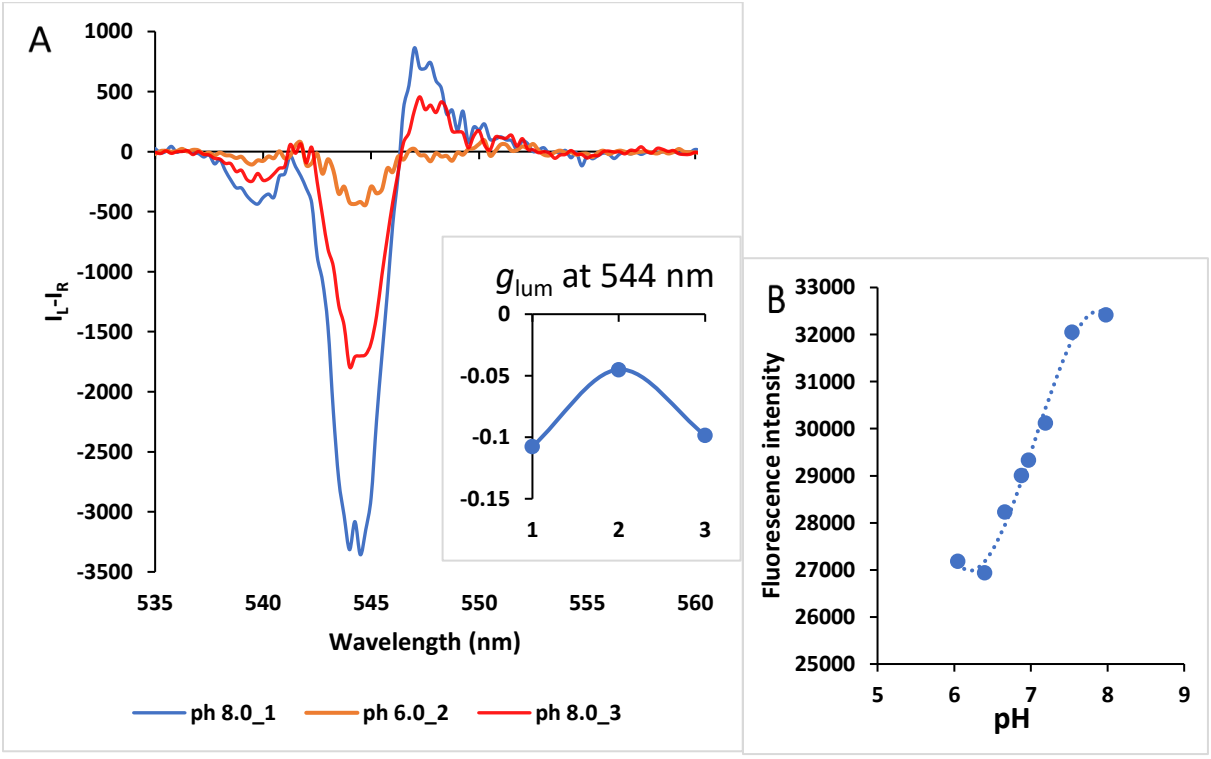

Figure S28: (a) Plot of CPL pH sensing reversibility of $[(S,S\text{-tpadac})Tb]^-_{(aq)}[K]^+_{(aq)}$ (5 μM in 0.1 M tris buffer) for $^5D_4 \rightarrow {}^7F_5$ transition. 295 nm excitation LED. Slit width 5 nm. Insert shows g_{lum} changes, (b) Plot of emission intensity (120 μM in tris buffer) at 544 nm against pH from which pKa was determined.

Metal Titration

General Procedure: A 2 mL volume of a 6.13 x 10^{-5} M solution of $[(S,S\text{-tpadac})Tb]^{-}_{(aq)}[K]^{+}_{(aq)}$ in 0.1 M tris buffer (pH 7.4) was measured into a quartz cuvette. Then incremental amounts (2 µL, that is 0.1 equivalent) of a 6.13 x 10^{-3} M aqueous solution of the metal salt ($Pb(OAc)_2$, $Cd(OAc)_2$, $MnBr_2$) was added using a micro-syringe and the CPL measured after each addition. This was repeated until 8 equivalents of the metal salt solution have been added. Aqueous solution of dipotassium EDTA was titrated to determine reversibility.

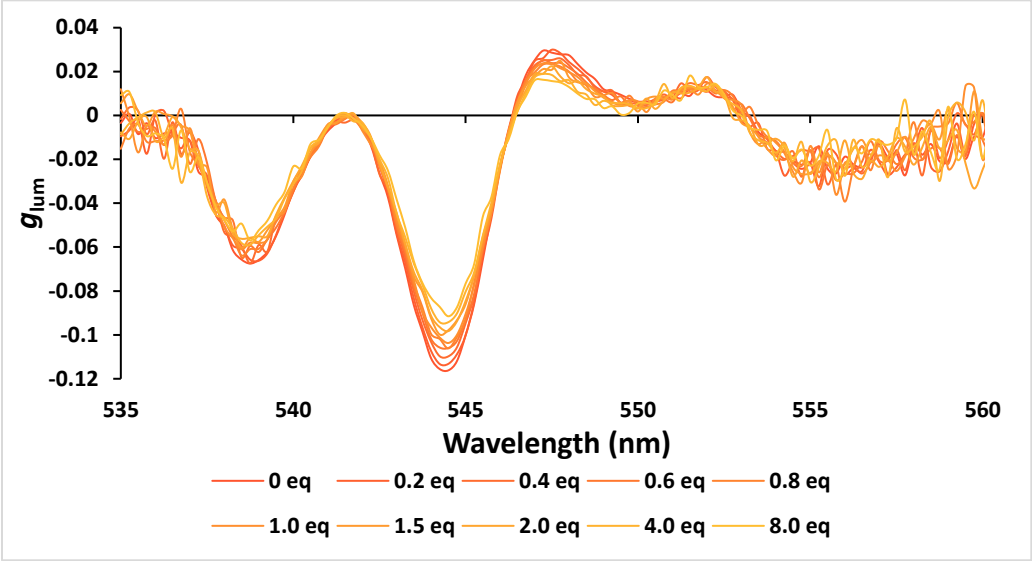

Figure S29: g_{lum} plot for titration of $[(S,S\text{-tpadac})Tb]^{-}_{(aq)}[K]^{+}_{(aq)}$ (6.13 x 10^{-5} M in 0.1 M tris buffer, pH 7.4) against Pb^{2+} for $^5D_4 \rightarrow {}^7F_5$ transition of Tb. 295 nm excitation LED. Slit width 2.4 nm.

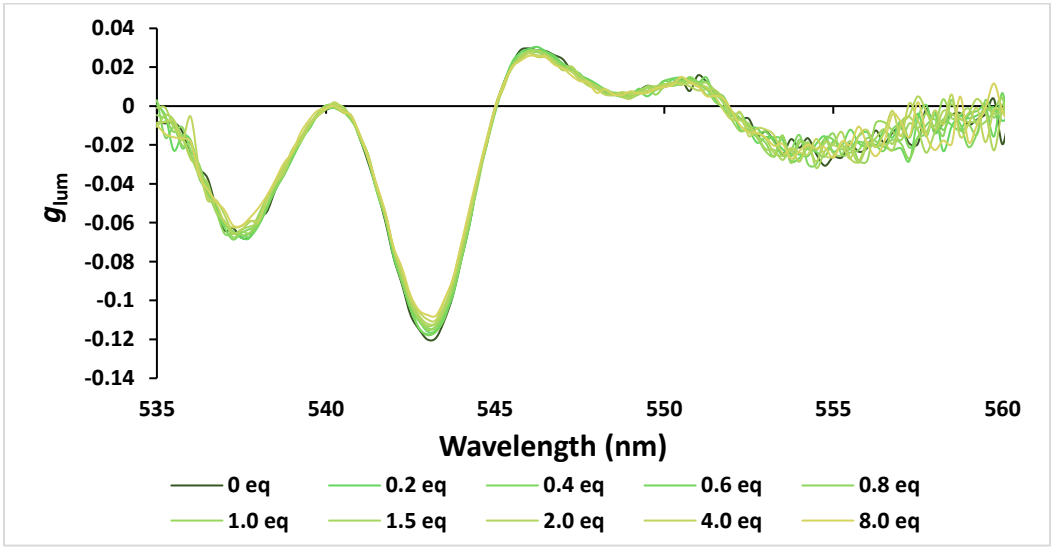

Figure S30: g_{lum} plot of titration of $[(S,S\text{-tpadac})Tb]^{-}_{(aq)}[K]^{+}_{(aq)}$ (6.1 x 10^{-5} M in 0.1 M tris buffer, pH 7.4) against Cd^{2+} for $^5D_4 \rightarrow {}^7F_5$ transition of Tb. 295 nm excitation LED. Slit width 2.4 nm.

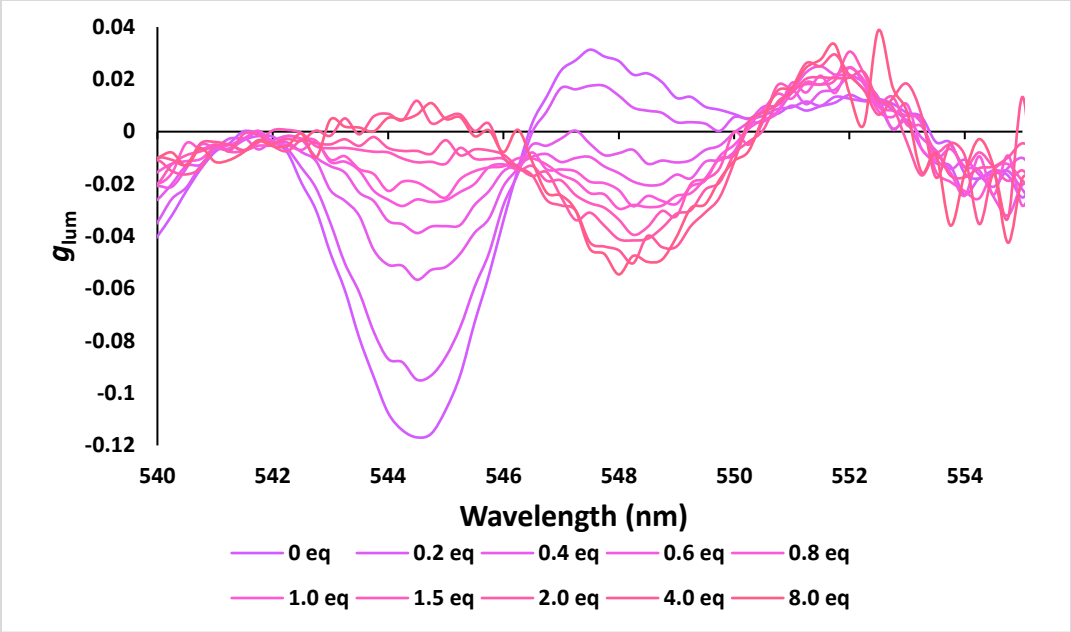

Figure S31: g_{lum} plot of titration of $[(S,S\text{-tpadac})Tb]^-_{(aq)}[K]^+_{(aq)}$ (6.1 x 10^{-5} M in 0.1 M tris buffer, pH 7.4) against Mn^{2+} for $^5D_4 \rightarrow {}^7F_5$ transition of Tb. 295 nm excitation LED. Slit width 2.4 nm.

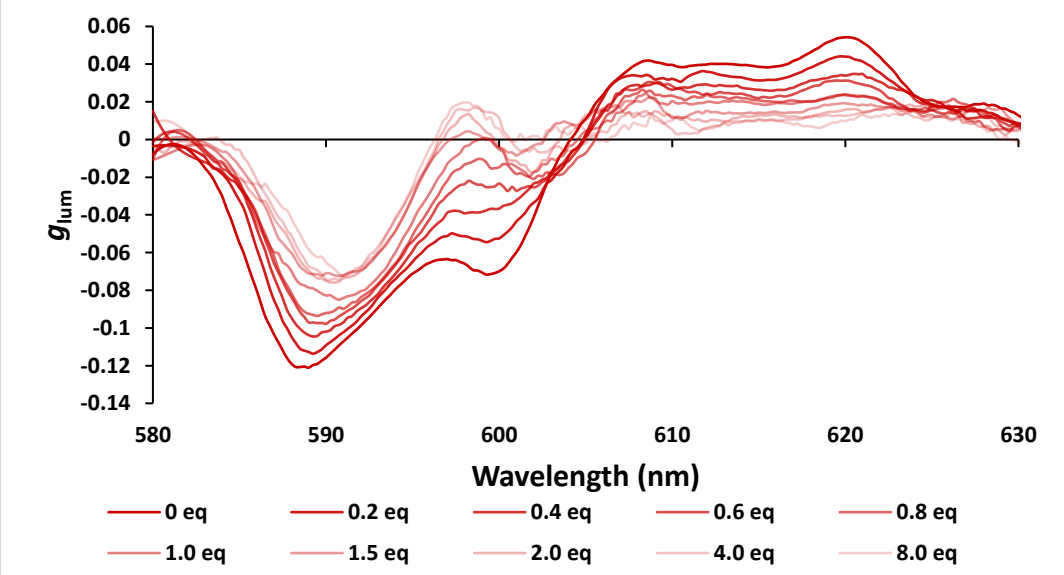

Figure S32: g_{lum} plot of titration of $[(S,S\text{-tpadac})Eu]^-_{(aq)}[K]^+_{(aq)}$ (6.1 x 10^{-5} M in 0.1 M tris buffer, pH 7.4) against Mn^{2+} for $^5D_0 \rightarrow {}^7F_1$ and $^5D_0 \rightarrow {}^7F_2$ transitions of Eu. 295 nm excitation LED. Slit width 5 nm.

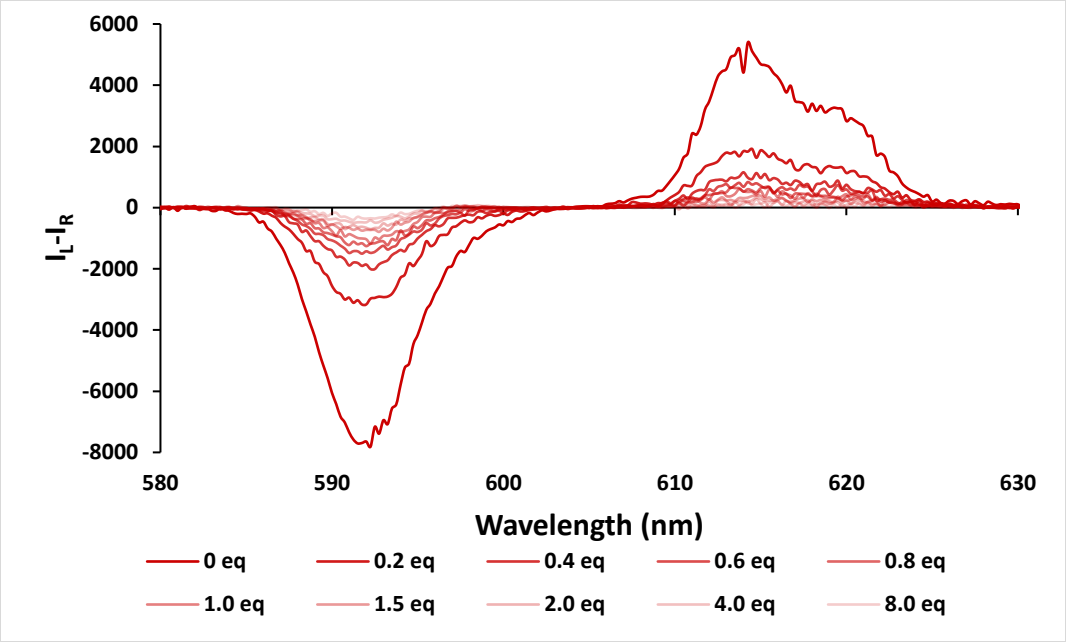

Figure S33: Δ*I* plot of titration of $[(S,S\text{-tpadac})Eu]^-_{(aq)}[K]^+_{(aq)}$ (6.1 x 10^{-5} M in 0.1 M tris buffer, pH 7.4) against Mn^{2+} for $^5D_0 \rightarrow {}^7F_1$ and $^5D_0 \rightarrow {}^7F_2$ transitions of Eu. 295 nm excitation LED. Slit width 5 nm.

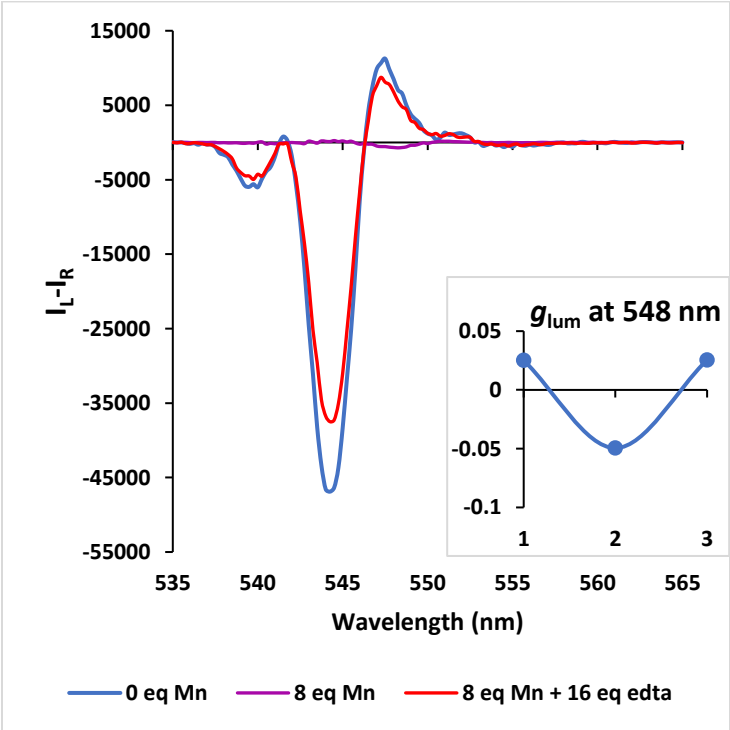

Figure S34: Plot of CPL Mn sensing reversibility of $[(S,S\text{-tpadac})Tb]^-_{(aq)}[K]^+_{(aq)}$ (60 μM in 0.1 M tris buffer) using dipotassium EDTA for $^5D_4 \rightarrow {}^7F_5$ transition. 295 nm excitation LED. Slit width 5 nm. Insert shows g_{lum} changes.

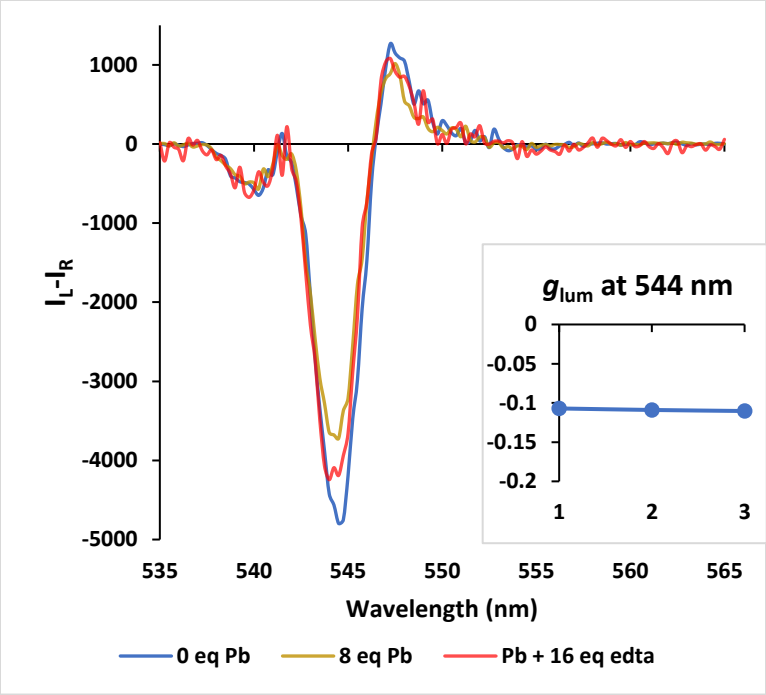

Figure S35: Plot of CPL Pb sensing reversibility of $[(S,S\text{-tpadac})Tb]^-_{(aq)}[K]^+_{(aq)}$ (5 μM in 0.1 M tris buffer) using dipotassium EDTA for $^5D_4 \rightarrow {}^7F_5$ transition. 295 nm excitation LED. Slit width 5 nm. Insert shows g_{lum} changes.

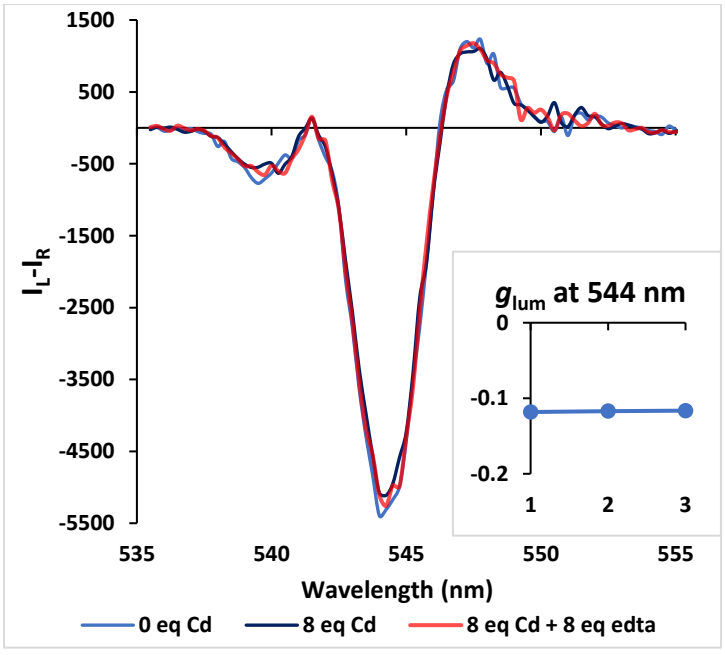

Figure S36: Plot of CPL Cd sensing reversibility of $[(S,S\text{-tpadac})Tb]^-_{(aq)}[K]^+_{(aq)}$ (5 μM in 0.1 M tris buffer) using dipotassium EDTA for $^5D_4 \rightarrow {}^7F_5$ transition. 295 nm excitation LED. Slit width 5 nm. Insert shows g_{lum} changes.

Lifetime Plots

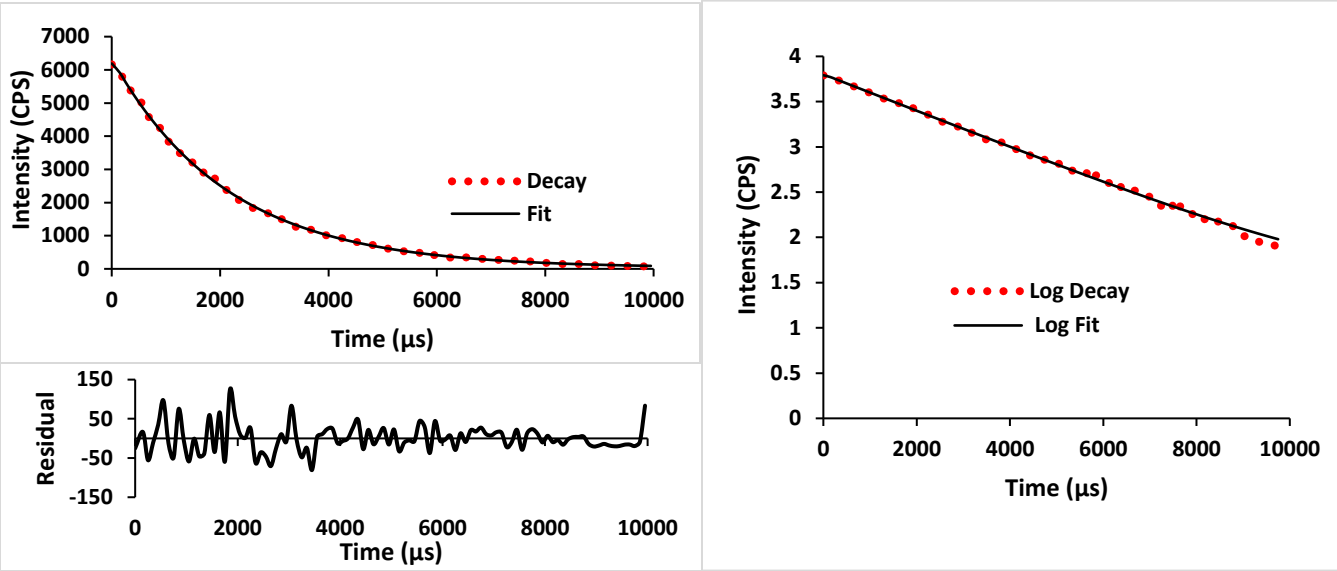

Figure S37: Lifetime exponential (left) and log (right) plots of [(*R*,*R*-tpadac)Tb]$^{-}_{(aq)}$[K]$^{+}_{(aq)}$ complex in 0.1 M tris buffer (pH 7.4, 298 K) for 544 nm. Excited with 280 nm LED, gate width of 4800 (10,000 µs window), 1000 µs delay, 1000 µs LED pulse width, and 500 events with a total cycle time of 11,000 µs. Plot is an average of 20 runs (τ_{obs} = 3.22 ms). The lifetime of the enantiomer is identical as expected.

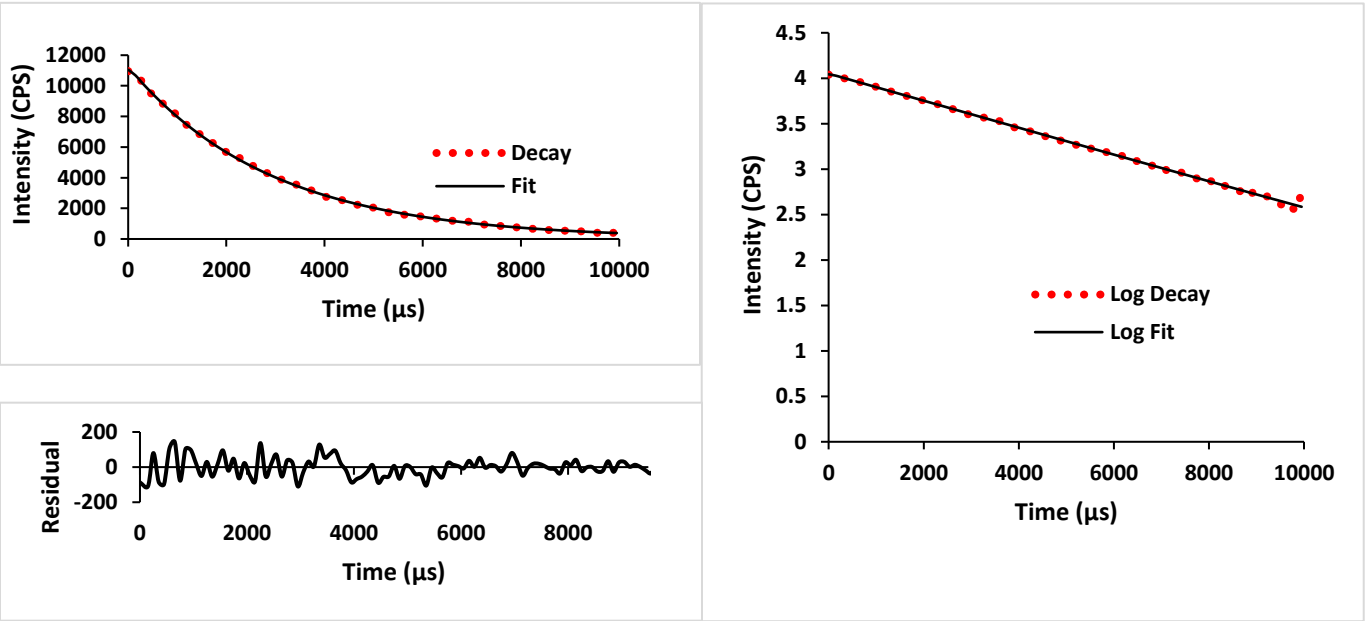

Figure S38: Lifetime exponential (left) and log (right) plots of [(*R*,*R*-tpadac)Tb]$^{-}_{(aq)}$[K]$^{+}_{(aq)}$ complex in D_2O for 544 nm. Excited with 280 nm LED, gate width of 4800 (10,000 µs window), 1000 µs delay, 1000 µs LED pulse width, and 500 events with a total cycle time of 11,000 µs. Plot is an average of 20 runs (τ_{obs} = 4.37 ms). The lifetime of the enantiomer is identical as expected.

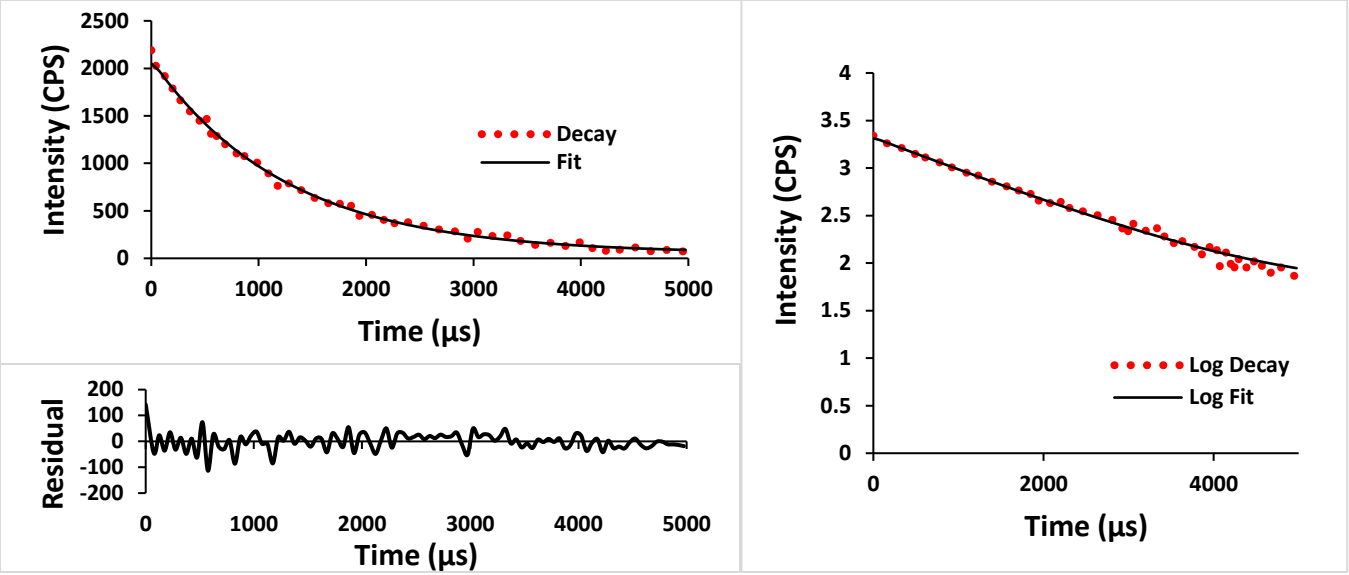

Figure S39: Lifetime exponential (left) and log (right) plots of $[(S,S\text{-tpadac})Eu]^-_{(aq)}[K]^+_{(aq)}$ complex in 0.1 M tris buffer (pH 7.4, 298 K) for 615 nm. Excited with 280 nm LED, gate width of 2400 (5,000 µs window), 1000 µs delay, 1000 µs LED pulse width, and 500 events with a total cycle time of 6,000 µs. Plot is an average of 20 runs (τ_{obs} = 1.88 ms). The lifetime of the enantiomer is identical as expected.

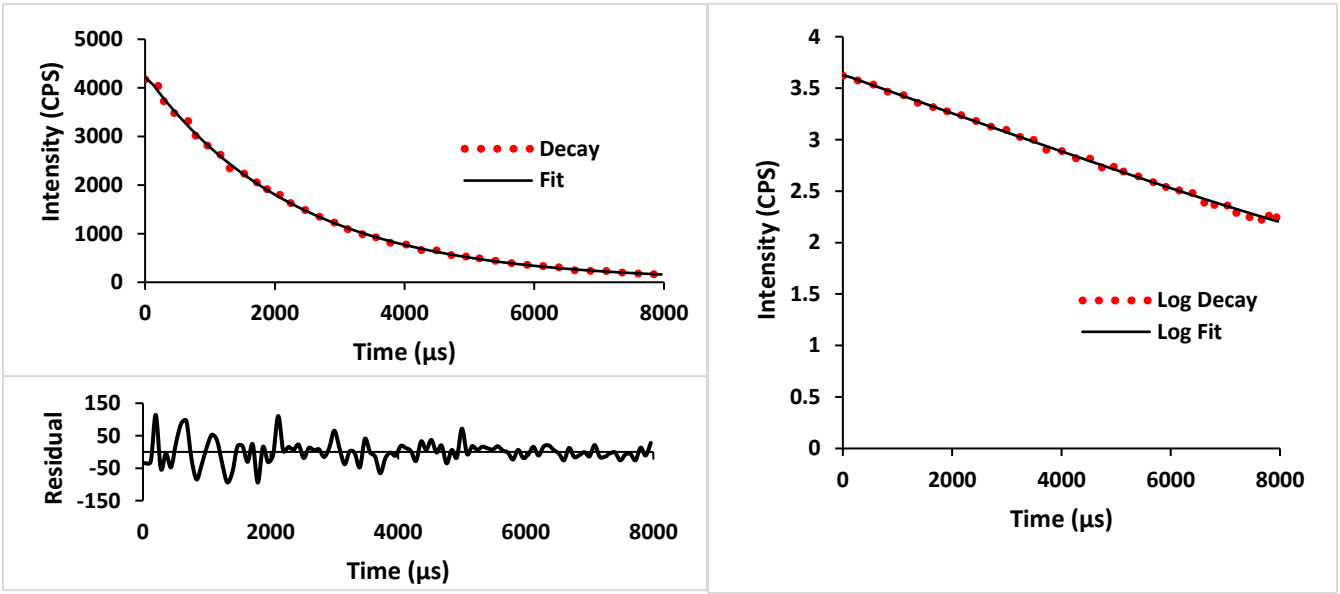

Figure S40: Lifetime exponential (left) and log (right) plots of $[(R,R\text{-tpadac})Eu]^-_{(aq)}[K]^+_{(aq)}$ complex in D_2O for 615 nm. Excited with 280 nm LED, gate width of 2400 (5,000 µs window), 1000 µs delay, 1000 µs LED pulse width, and 500 events with a total cycle time of 6,000 µs. Plot is an average of 20 runs (τ_{obs} = 3.43 ms). The lifetime of the enantiomer is identical as expected.

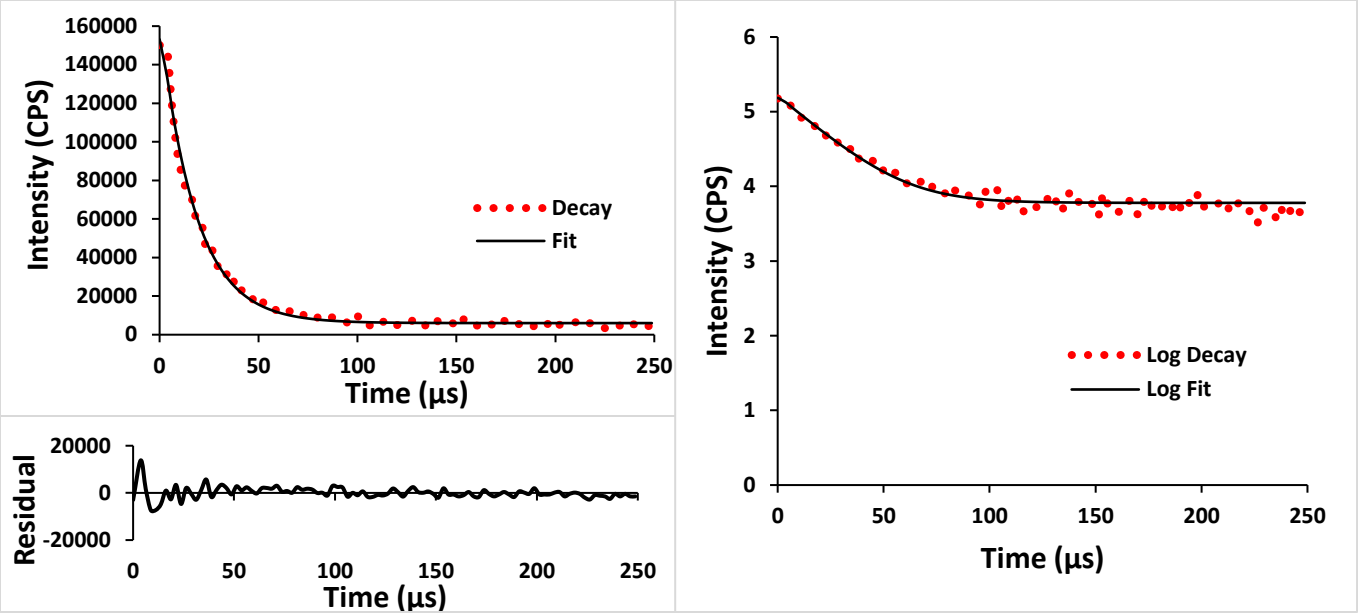

Figure S41: Lifetime exponential (left) and log (right) plots of [(*R*,*R*-tpadac)Dy]$^{-}_{(aq)}$[K]$^{+}_{(aq)}$ complex in 0.1 M tris buffer (pH 7.4, 298 K) for 480 nm. Excited with 280 nm LED, gate width of 120 (250 µs window), 500 µs delay, 500 µs LED pulse width, and 1500 events with a total cycle time of 750 µs. Plot is an average of 35 runs for better resolution (τ_{obs} = 0.026 ms). The lifetime of the enantiomer is identical as expected.

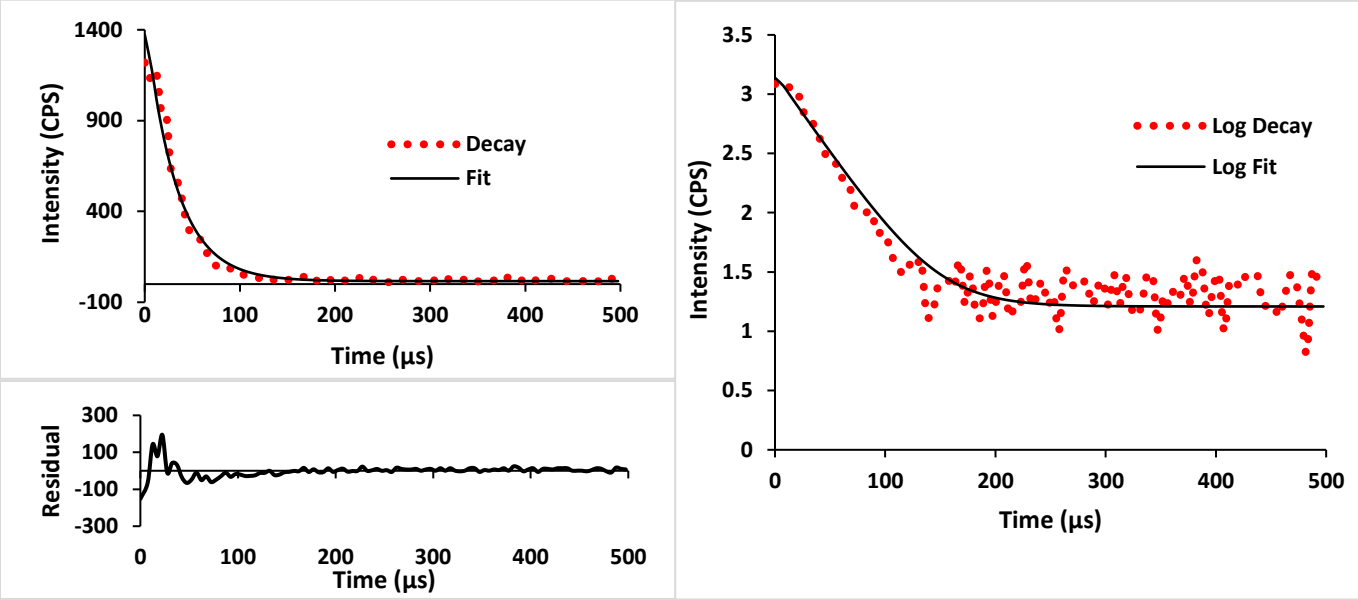

Figure S42: Lifetime exponential (left) and log (right) plots of [(*S*,*S*-tpadac)Sm]$^{-}_{(aq)}$[K]$^{+}_{(aq)}$ complex in 0.1 M tris buffer (pH 7.4, 298 K) for 596 nm. Excited with 280 nm LED, gate width of 240 (500 µs window), 480 µs delay, 500 µs LED pulse width, and 1500 events with a total cycle time of 1500 µs. Plot is an average of 40 runs for better resolution (τ_{obs} = 0.048 ms). The lifetime of the enantiomer is identical as expected.

Crystallographic Information
Crystal Table for [(*S*,*S*-tpadac)Eu][K]

Table S2: Summary of Crystallographic Parameters

Identification code	JA252 [(*S*,*S*-tpadac)Eu][K]
Empirical formula	$C_{34}H_{40}EuKN_6O_{14}$
Formula weight	947.88
Temperature/K	100.01(10)
Crystal system	Monoclinic
Space group	C2
a/Å	15.29779(11)
b/Å	21.15984(14)
c/Å	12.02910(9)
α/°	90
β/°	101.9753(7)
γ/°	90
Volume/Å^3	3809.06(5)
Z	4
ρ_{calc}g/cm^3	1.653
μ/mm^{-1}	13.421
F(000)	1920.0
Crystal size/mm^3	0.258 × 0.149 × 0.105
Radiation	CuKα (λ = 1.54184)
2Θ range for data collection/°	7.236 to 143.24
Index ranges	$-18 \leq h \leq 18$, $-25 \leq k \leq 25$, $-14 \leq l \leq 14$
Reflections collected	28717
Independent reflections	7354 [R_{int} = 0.0307, R_{sigma} = 0.0252]
Data/restraints/parameters	7354/57/523
Goodness-of-fit on F^2	1.073
Final R indexes [I>=2σ (I)]	R_1 = 0.0395, wR_2 = 0.1060
Final R indexes [all data]	R_1 = 0.0402, wR_2 = 0.1065
Largest diff. peak/hole / e Å^{-3}	1.82/-1.31
Flack parameter	0.004(3)

Reference

N. Chatterton, Y. Bretonniere, J. Pecaut and M. Mazzanti. An efficient design for the rigid assembly of four bidentate chromophores in water-stable highly luminescent lanthanide complexes. *Angew. Chem. Int. Ed.*, 2005, **44**, 7595-7598.